HHMI Author Manuscript

HHMI Author Manuscript

HHMI Author Manuscript

Howard Hughes Medical Institute

Published as: *Methods Enzymol*. 2016 ; 572: 1–49.

RNA Imaging with Multiplexed Error Robust Fluorescence in situ Hybridization

Jeffrey R. Moffitt[1,*] and **Xiaowei Zhuang**[1,2,*]

[1]Howard Hughes Medical Institute, Department of Chemistry and Chemical Biology, Harvard University, Cambridge, Massachusetts, 02138 USA

[2]Department of Physics, Harvard University, Cambridge, Massachusetts, 02138 USA

Abstract

Quantitative measurements of both the copy number and spatial distribution of large fractions of the transcriptome in single-cells could revolutionize our understanding of a variety of cellular and tissue behaviors in both healthy and diseased states. Single-molecule Fluorescence *In Situ* Hybridization (smFISH)—an approach where individual RNAs are labeled with fluorescent probes and imaged in their native cellular and tissue context—provides both the copy number and spatial context of RNAs but has been limited in the number of RNA species that can be measured simultaneously. Here we describe Multiplexed Error Robust Fluorescence *In Situ* Hybridization (MERFISH), a massively parallelized form of smFISH that can image and identify hundreds to thousands of different RNA species simultaneously with high accuracy in individual cells in their native spatial context. We provide detailed protocols on all aspects of MERFISH, including probe design, data collection, and data analysis to allow interested laboratories to perform MERFISH measurements themselves.

1. Introduction

In situ hybridization of fluorescently labeled oligonucleotide probes to cellular RNAs has emerged as a powerful technique for the quantification of both the copy number of individual transcripts and the spatial distribution of these molecules within single cells (Femino et al., 1998; Raj et al., 2008). In this approach, cells are fixed and permeabilized, and a small number of fluorescently labeled oligonucleotide probes, whose sequences are complementary to different regions of the RNA of interest, are introduced into the cell. Basepairing between these probes and their target RNA favors specific binding of these probes to their target, and the use of multiple probes per target concentrates many probes within the small volume of the cell occupied by each copy of that RNA, producing bright fluorescent spots that can be distinguished from cellular background and stray probes. These spots can then be counted to determine the copy number of the RNA of interest and their locations within individual cells and intact tissues.

*Correspondence: lmoffitt@mcb.harvard.edu, zhuang@chemistry.harvard.edu.

NanoString Exhibit 1021.001

HHMI Author Manuscript

HHMI Author Manuscript

HHMI Author Manuscript

With these technical abilities, smFISH has emerged as a powerful tool in the study of a wide range of questions in cellular and tissue biology. For example, the ability to quantify the copy number of individual RNAs within single cells has driven a variety of exciting advances in our understanding of the natural cell-to-cell variation in gene expression within homogenous populations of cells as well as the expression differences which correlate with and likely drive the development of complex cell types within tissues (Larson et al., 2009; Munsky et al., 2012; Padovan-Merhar and Raj, 2013; Raj and van Oudenaarden, 2008; Sanchez and Golding, 2013). Similarly, the ability to precisely image the spatial distribution of different RNAs within cells has revealed that the transcriptome of many cells types is spatially organized. Remarkably, this organization has emerged as an important regulator of a broad range of cellular phenotypes, from directional crawling of individual cells to the establishment of body plan in multicellular organisms (Balagopal and Parker, 2009; Besse and Ephrussi, 2008; Buxbaum et al., 2014; Holt and Schuman, 2013; Lécuyer et al., 2009; Martin and Ephrussi, 2009; Rodriguez et al., 2008; St Johnston, 2005).

However, the number of RNA species that can be simultaneously imaged by smFISH has been limited. Most experiments stain and image only one RNA species at a time, and even the most advanced multiplexing efforts have only extended this approach to the simultaneous measurement of ~10–30 RNA species (Jakt et al., 2013; Levesque and Raj, 2013; Levsky et al., 2002; Lubeck and Cai, 2012; Lubeck et al., 2014). However, many interesting questions require much higher levels of multiplexing—levels that approach the transcriptome scale. For example, comprehensive or hypothesis-free studies of gene regulatory networks, transcriptional definitions of cell type, or systematic screens for cell-type markers, could all benefit from precise copy number measurement of hundreds to thousands of RNAs, if not the entire transcriptome, simultaneously within single cells. Similarly, efforts to systematic map the spatial organization of the transcriptome, to determine the molecular transport mechanisms that establish and dynamically regulate this spatial organization, and to elucidate the ultimate role that this organization plays in post-transcriptional regulation, would also benefit from the ability to map the spatial organization of large fractions of the transcriptome simultaneously within single cells.

To address this technical demand, we recently introduced a massively multiplexed smFISH imaging method that extends the benefits of this powerful technique towards the transcriptome-scale. We term this approach Multiplexed, Error-Robust, Fluorescence *In Situ* Hybridization (MERFISH) (Chen et al., 2015). MERFISH achieves large-scale multiplexing by assigning error-robust barcodes to different RNA species and then reading out these barcodes through successive rounds of hybridization and imaging on the same sample. In Section 2 of this chapter, we provide a more detailed discussion of the conceptual challenges to multiplexing smFISH, the way in which MERFISH addresses these challenges, and the published performance of MERFISH. In the subsequent sections, we provide detailed instructions, protocols, and tips on how to perform a MERFISH measurement, including details on how to design oligonucleotide probes (Section 3), how to construct these probes (Section 4), how to prepare samples (Section 5), how to execute a MERFISH measurement (Section 6), and, finally, how to analyze MERFISH data (Section 7). In many ways, MERFISH is only moderately more complicated than smFISH, and the goal of this chapter is to provide protocols and advice that will allow interested laboratories to perform

NanoString Exhibit 1021.002

HHMI Author Manuscript

HHMI Author Manuscript

HHMI Author Manuscript

MERFISH measurements themselves. As MERFISH is based on smFISH, we also recommend several reviews on smFISH for readers to learn about the basics of smFISH measurements (Batish et al., 2011; Itzkovitz and van Oudenaarden, 2011; Youk et al., 2010; Zenklusen and Singer, 2010).

2. MERFISH Overview

2.1. Combinatorial Barcoding and Sequential Readout

MERFISH significantly increases the multiplexing of smFISH measurements by utilizing a combinatorial labeling approach to associate unique barcodes with individual RNA species and then by reading out these barcodes through a series of sequential hybridization and imaging measurements. Combinatorial labeling approaches have been utilized previously to increase the multiplexing of smFISH measurements (Jakt et al., 2013; Levesque and Raj, 2013; Levsky et al., 2002; Lubeck and Cai, 2012). In these approaches, each RNA species is often identified not by a single color of fluorescently labeled smFISH probe but rather with a unique combination or `barcode' of colors. For example, one RNA might be identified by red-labeled probes alone while another might be identified by the combination of red-, green-, and blue-labeled probes. We can formalize this discussion by adopting a binary representation of this barcoding scheme with the presence or absence of a color being represented by a `1' or `0', respectively, within a given bit. For example, a red-labeled RNA might be represented as 100 while an RNA labeled with all three colors would be represented by 111. In this example, three colors implies three bits which, in turn, implies 2^3=8 possible color combinations. This geometric scaling between the number of unique barcodes and the number of measured labels (i.e. bits or colors) is what makes combinatorial labeling such a powerful approach to multiplexing.

However, to significantly increase the multiplexing of smFISH measurements, far more than three distinguishable colors would be needed. For example, the simultaneous identification of 1000 RNA species would require at least 10 colors! Unfortunately, distinguishing such a large number of colors via optical microscopy can be quite challenging. For this reason, MERFISH adopts an alternative approach: Instead of measuring binary barcodes with different color combinations, each bit in the binary barcode is determined by the presence or absence of fluorescence in a single round of hybridization and imaging (Chen et al., 2015). Simply put, the barcode is built up one bit at a time via a series of smFISH measurements, all on the same sample. Figure 1A illustrates the conceptual approach. In the first round, a subset of RNAs are stained. If fluorescent in this round, an RNA is assigned a `1' in the first bit. If it is not fluorescent, it is assigned a `0'. A second set of probes is then hybridized to the same sample, and this sample is imaged again. Each RNA is then assigned a `1' or `0' in the *second* bit based on whether or not it is fluorescent in this second round of smFISH. This process is repeated across N rounds of smFISH imaging, allowing the construction of an N-bit barcode for each labeled RNA in the sample. These binary barcodes can then be used to identify the species of each labeled RNA. By adopting a sequential hybridization and imaging readout approach, as opposed to a colorimetric readout approach, it is possible to imagine identifying very large numbers of RNAs within a single sample (Chen et al., 2015). See Figure 1B. For example, only 16 rounds of hybridization and imaging would be required

NanoString Exhibit 1021.003

HHMI Author Manuscript

HHMI Author Manuscript

HHMI Author Manuscript

to generate enough unique barcodes — ~65,000 — to identify most if not all of the expressed RNA species within individual human cells! We note that a different approach to take advantage of color barcodes and sequential imaging to increase the number detectable RNA species has also been proposed, though in the reported experimental demonstration of this approach, the number of RNA species imaged in individual cells is still on the order of ~10-20 (Lubeck et al., 2014).

2.2. Error Robust and Correcting Codes

In practice, a substantial limitation to multiplexing arises from the small readout errors that are inherent to smFISH. There are two such errors. First, occasionally an RNA that should fluoresce in one imaging round does not accumulate enough fluorescently labeled probe to produce a bright enough signal to be called as an RNA. Second, stray probes or a bright autofluorescent spot in the cell can sometimes produce a spot bright enough to be called an RNA when it is not. In the context of reading out a binary barcode, these errors would correspond to misreading a `1' as a `0' or a `0' as a `1', respectively.

Such errors are infrequent— `1' to `0' errors typically occur at frequencies of ~10% while `0' to `1' errors occur a few-fold less frequently—and, thus, have little effect on the performance of traditional smFISH measurements (Raj et al., 2008). However, in combinatorial barcoding approaches, such as MERFISH, the effect of these errors compounds quickly as the length of the barcode increases, producing two forms of measurement errors (Chen et al., 2015). See Figure 1C and D. First, the probability that no measurement errors are made during barcode readout drops with each additional bit in the barcode and, thus, the fraction of barcodes measured correctly—what we term the *calling rate*—decreases with increasing barcode length. More problematically, each readout error transforms one barcode into another, and such errors can lead to the misidentification of one RNA as another. As the length of the barcode increases, the rate at which RNAs are incorrectly identified—what we term the *misidentification rate*—increases quickly. Thus, while it is theoretically possible to measure enough barcodes to identify the entire human transcriptome in just 16 rounds of imaging, even with modest readout errors, the vast majority of these RNAs would be identified incorrectly!

To address this problem, we sought to use error-robust or error-correcting encoding schemes in MERFISH (Chen et al., 2015). The idea behind these encoding schemes is quite simple: Instead of assigning each possible binary barcode to a RNA, many of the possible binary barcodes are left unassigned (Moon, 2005). If one of these unassigned barcodes is observed, then it is clear that an error has occurred. The Hamming Distance (HD) between two barcodes—the number of bits that must be switched to convert one barcode into another—is a useful concept in understanding the behaviors of these encoding schemes (Moon, 2005). If, out of all possible binary barcodes, only barcodes that are separated by at least a HD of 2 are used, then no single-bit readout error can transform one barcode into another, reducing the misidentification rate. Further increasing the minimum HD between used barcodes by leaving more possible barcodes unassigned will produce even larger reductions in the misidentification rate. See Figure 1D. In addition to a reduction in the misidentification rate, some encoding schemes can also improve the calling rate through a process known as error

NanoString Exhibit 1021.004

HHMI Author Manuscript

HHMI Author Manuscript

HHMI Author Manuscript

correction. Consider an encoding scheme in which the minimum HD between all barcodes is 4. If a single error occurs in the readout of a barcode, it will produce a barcode with a HD of 1 from the actual correct barcode but a HD of at least 3 from all other possible barcodes. Thus, the measured barcode can not only be recognized as containing an error, it can also be associated with the correct barcode with reasonable certainty. The result, as illustrated in Figure 1C, is a significant increase in the calling rate.

In the typical smFISH measurement the rate at which a `1' is misread as a `0' is often several-fold larger than the rate of misreading a `0' as a `1'. If left unaddressed, this asymmetry would introduce bias into measurements (Chen et al., 2015). Specifically, barcodes that contain more `1's than other barcodes would tend to have more errors and would thus be prone to a lower calling rate and a higher misidentification rate than barcodes that contain fewer `1's. We address this potential bias with encoding schemes known as constant Hamming Weight codes (Chen et al., 2015). (The Hamming Weight is defined as the number of `1's in a binary barcode). In such codes, the only binary barcodes that are used are barcodes that have the same Hamming Weight, e.g. only barcodes with four `1's are used. Because of the asymmetries in error rates, the use of a low Hamming Weight code can remove barcodes subject to higher frequency of errors and, thus, raises calling rates and lowers misidentification rates, as seen in Figure 1C and D.

2.3. Two Stage Hybridization

Hybridization time is a significant challenge for an approach that adopts a sequential hybridization and imaging approach to readout barcodes. This challenge arises from the observation that hybridization of DNA oligonucleotides to cellular RNA is a slow process, typically requiring 6–24 hours for efficient labeling (Shaffer et al., 2013) because sequences on the cellular RNAs could be occluded by base-pairing with other sequences or by binding of proteins. Thus, with typical hybridization approaches, measuring a 16-bit barcode could require nearly two weeks! To solve this problem, we perform two types of hybridizations in MERFISH (Chen et al., 2015). In the first hybridization, we stain the sample with single-stranded DNA oligonucleotides that we term *encoding probes*. See Figure 2. These probes contain two types of hybridization regions. The first region is termed the *targeting region*, and it is complementary to the sequence of a specific RNA of interest, allowing the encoding probes to hybridize to the target RNA of interest with high efficiency and specificity. The second region is termed the *readout region*. It is comprised of one or more custom sequences that are complementary to fluorescently-labeled readout probes, again designed to bind with high efficiency and specificity to the complementary readout sequence. See Figure 2. Binding of the encoding probes to cellular RNA is a slow process, requiring at least 12 hours of hybridization. But once this slow hybridization is complete, we found that the hybridization necessary to read each readout sequence in the barcode with readout probes can be completed much more quickly, presumably because the readout sequences are not occluded by the binding of any cellular proteins or RNA. Thus, what might have been a two-week long experiment can be accomplished in under 12 hours. Figure 2 depicts the multiple hybridization rounds required for the typical MERFISH measurement.

NanoString Exhibit 1021.005

HHMI Author Manuscript

HHMI Author Manuscript

HHMI Author Manuscript

2.4. Performance of MERFISH

In our published proof of principle for MERFISH, we demonstrated the ability to measure 140 or 1,001 RNA species simultaneously in individual cells using two different encoding schemes (Chen et al., 2015). Using an encoding scheme with 16-bit barcodes separated by a minimum HD of 4 and with a uniform Hamming Weight of 4, we demonstrated that we could identify 140 RNA species simultaneously in individual cells with accuracy and efficiency very similar to those demonstrated for smFISH. We term this encoding scheme a modified Hamming Distance 4 code (MHD4). Figure 3A–D illustrates the use of this approach to image RNAs in human fibroblast cells (IMR90s). Control measurements in these cells revealed little technical bias, i.e. the measured copy number for each RNA species did not depend on the binary barcode that had been assigned to it (Figure 3E). Moreover, we observed excellent agreement between copy numbers as determined by MERFISH and bulk-sequencing, with a Pearson correlation coefficient between the logarithmic abundances measured by these two techniques of 0.89 (Figure 3F). Finally, we compared the copy numbers as determined by MERFISH to those determined by traditional smFISH for 15 different RNAs that span an abundance range that covers nearly three orders of magnitude (Figure 3G). We also observed excellent correlation between these measurements and those of MERFISH; however, on average, MERFISH counted slightly smaller numbers of RNAs than that counted by traditional smFISH, roughly 80%. This slight reduction in calling rate is as expected given the measured per-bit 1-to-0 and 0-to-1 errors (Figure 1C, magenta). The excellent agreement between MERFISH measurements and smFISH extended even to lowest abundance ranges, < 1 copy per cell on average, revealing that the detection limit of MERFISH must be better than 1 RNA copy per cell.

To demonstrate the ability to further increase the multiplexing of smFISH measurements, we also tested a different encoding scheme capable of detecting but not correcting errors (Chen et al., 2015). Specifically, we used an encoding scheme with 14-bit barcodes separated by at least a HD of 2 and with a constant Hamming Weight of 4. The inability to correct errors was predicted to lower our calling rate. Indeed, we observed that the calling rate with this encoding scheme dropped to ~25%, as determined by comparing the measured copy numbers to those determined for individual RNAs using smFISH. However, this modified Hamming Distance 2 code (MHD2) encoding scheme still provided fairly accurate RNA measurements as evidenced by high Pearson correlation coefficients between these MERFISH measurements and bulk sequencing (0.76) as well as between these measurements and the subset of RNAs also measured via MERFISH with the higher accuracy MHD4 code (0.89). We anticipate that it should also be possible to measure ~1000 genes with our MHD4 code by using more rounds of imaging or utilizing multiple colors to readout multiple bits in each round of hybridization, for example, a 32-bit MHD4 code with a Hamming weight of 4 can encode ~1200 RNAs.

In summary, the performance of MERFISH can be tuned to the demands of the experiment through judicious choice of the properties of the encoding scheme. If very high performance —comparable to smFISH—is required, than an encoding scheme capable of identifying and correcting errors is probably the appropriate choice. Whereas if a reduced calling rate and modest reduction in the accuracy of the measurement are tolerable, than much higher

NanoString Exhibit 1021.006

HHMI Author Manuscript

HHMI Author Manuscript

HHMI Author Manuscript

multiplexing for a fixed number of bits can also be achieved using an encoding scheme that can identify but not correct errors.

3. The Design of Oligonucleotide Probes

The first step in any MERFISH experiment is the design of the oligonucleotide probes that will be used to label individual RNA species. In our current implementation of MERFISH, each oligonucleotide encoding probe consists of three basic components as illustrated in Figure 2. The first region is a 30-nt targeting region that is complementary to a portion of the sequence of the RNA to which it is designed to bind. The second region is a set of sequences that are called readout sequences, which were designed to be complementary and hence only bind to MERFISH readout probes and not other nucleic acid in the cell. Finally, the third region is a set of priming regions used in the construction of these probes, which will be discussed in detail in Section 4. In addition to the nucleotide sequences for each of these components, a *codebook*—the specific set of binary barcodes that will be used and their association with different RNA species of interest—must also be designed. In this section, we provide protocols to design these sequences and to build a codebook. Example code to perform these steps can be found at http://zhuang.harvard.edu/merfish/.

3.1. Design of Target Regions

Functionally, the goal of a target region is to direct the binding of each encoding probe to its target RNA of interest with high binding efficiency and specificity. The central challenge in the design of target regions for MERFISH (and smFISH, in general), is to design a set of target regions where these properties are optimized for all probes under a constant set of hybridization conditions, e.g. incubation temperature. To accomplish this goal target regions are designed to cover a relatively narrow range of GC content and melting temperatures (T_M) with their target. In addition, a good target region should have limited homology to other RNAs in the transcriptome, reducing the probability that it will bind to the wrong RNA. Finally, the typical smFISH measurement does not bind each RNA with a single probe but rather tiles that RNA with multiple probes, each of which targets a different portion of the sequence of the RNA. See Figure 2. For many smFISH measurements, the number of unique probes per RNA is often ~50; however, this number can be lowered with a corresponding reduction in the brightness of the individual RNA spots (Raj et al., 2008). For initial MERFISH work, we recommend having at least 50 encoding probes per RNA.

As described by others (Raj et al., 2008), smFISH probes can be designed online using a web interface (https://www.biosearchtech.com/support/tools/design-software/stellaris-probe-designer). In principle, probes designed with this software should work well as target regions for MERFISH. However, there is no batch processing option for such software and submitting hundreds to thousands of genes individually would be very labor intensive. Thus, we describe below the alternative approach that we have used.

We design our target regions with the software package, OligoArray 2.0, which was developed for the design of microarrays (Rouillard, 2003). This software has been used previously in the design of FISH probes for DNA (Beliveau et al., 2012). In addition to the ability to batch process mRNAs, one advantage of this software is the additional stringency

NanoString Exhibit 1021.007

HHMI Author Manuscript

HHMI Author Manuscript

HHMI Author Manuscript

OligoArray applies to the design of its probes. Specifically, internal secondary structure and off-target binding are assessed not via the number of complementary bases but by the thermodynamic stability of these structures. Of course these extra calculations come at a computational cost, and calculation of target regions for a large number of genes can take days of computing resources on a desktop computer.

Step 1: Download and install all necessary software. OligoArray2.0 can be downloaded from http://berry.engin.umich.edu/oligoarray2_1/. This software requires OligoArrayAux which can be downloaded from http://unafold.rna.albany.edu/?q=DINAMelt/OligoArrayAux. OligoArray2.0 will look for this software in a specific directory (C:\Program Files \OligoArrayAux\), so it must be installed there. Finally, OligoArray2.0 also requires several legacy BLAST functions, which can be downloaded and installed from http://blast.ncbi.nlm.nih.gov/Blast.cgi?CMD=Web&PAGE_TYPE=BlastDocs&DOC_TYPE=Download.

Step 2: Download a fasta file containing the transcriptome of interest. These files can be found from a variety of repositories, such as those hosted by NCBI, UCSC, or Ensembl. For example, the human transcriptome can be downloaded from Ensembl using the cDNA link found on this page: http://www.ensembl.org/info/data/ftp/index.html.

Step 3: Create a BLAST database of the transcriptome for OligoArray2.0 to identify potential off-target binding. Instructions on how to create this database using the legacy BLAST functionality can be found here http://blast.ncbi.nlm.nih.gov/Blast.cgi?CMD=Web&PAGE_TYPE=BlastDocs&DOC_TYPE=Download.

Step 4: Run OligoArray2.0 on the desired transcripts. OligoArray2.0 is a java based program and a full description of its use can be found here: http://berry.engin.umich.edu/oligoarray2_1/. When run, it must be supplied with a variety of parameters that place limits on the properties of the designed target regions, e.g. the length of possible probes, the suitable GC and melting temperature ranges, as well as the maximum T_M for potential off-target sequences. For the design of our target regions, we have used the following parameters: target region length of 30 nt; the T_M of the properly hybridized probe greater than 70° C; a lower bound on the T_M of hybridization to potential off-target sequences of 72° C; no internal secondary structure with a T_M lower than 76° C; and no contiguous run of the same nucleotide longer than six. These parameter ranges were selected to balance the demands for high stringency of probe binding with the design of enough distinct target regions to label each RNA.

Step 5: Parse the OligoArray output. OligoArray2.0 generates an output file, the details of which are described here: http://berry.engin.umich.edu/oligoarray2_1/. If a potential target region has homology to other transcripts, it will be indicated in this file. We only use potential target regions for which no potential off-targets were discovered.

Step 6: Repeat this process for all desired genes. As mentioned above, OligoArray2.0 is computationally intensive; thus, we recommend only using this software to design target regions for the desired subset of the transcriptome. Moreover, because computational cost does not grow linearly with the length of a transcript, we recommended that longer

NanoString Exhibit 1021.008

HHMI Author Manuscript

HHMI Author Manuscript

HHMI Author Manuscript

transcripts be split into smaller fragments and processed individually. We split transcripts into 1-kb increments.

3.2. Design of Readout Probes

There are several important considerations in the design of readout probes. First, to improve the binding efficiency of these probes, it is desirable to select probes that have similar T_M and GC content so that their hybridization properties are similar under a given hybridization condition. Second, to limit the number of potential off-target binding sites, potential sequences should be screened for homology to RNAs in the transcriptome of interest. Third, these sequences must be orthogonal, in that they should have limited homology with one another to prevent binding of one readout probe to the wrong readout sequence.

We have already screened and validated several readout probes for human samples, and we recommend the use of these sequences, which are provided in Table 1. The following steps can be taken if new or additional readout probes are required.

Step 1: Utilize existing sets of orthogonal nucleic acid sequences to design readout probes. It is important that one readout probe has little homology with a sequence of another probe to prevent potential off-target binding. Fortunately, a set of 25-mer nucleotide sequences designed to have limited cross homology exists, and we recommend using this resource to design readout sequences (Xu et al., 2009). These sequences can be downloaded from http://elledgelab.med.harvard.edu/?page_id=638. We have found good performance with readout sequences of 30-nt length, which can be created from these 25-nt sequences by either concatenating portions of them or adding 5 random nucleotides to either end.

Step 2: Remove potential probes with homology to members of the transcriptome of interest. To remove probes with significant homology to members of the transcriptome, we create a BLAST library to the transcriptome as described in Section 3.1 Step 3. We then BLAST each potential readout probe sequence against this library and remove any probe which contains a contiguous stretch of homology longer than 14 nt. This length was selected to balance the desire for shorter regions of homology with the increased frequency with which such shorter regions appear in the transcriptome.

Step 3: Remove potential readout probes with significant homology to one another. While these oligos were originally designed to have limited cross homology, changing their length may introduce new regions of homology. We recommend selecting a subset of possible readout probes, building a BLAST database for these sequences, and then use BLAST to identify regions of homology, as described in Step 2. We exclude probes that contain a region of homology to another potential probe longer than 10 nt.

Step 4: Order these probes. We order probes from IDT (www.idtdna.com) tagged on the 3' end with a Cy5. We have them synthesized on the 100 nmole synthesis scale and HPLC purified.

NanoString Exhibit 1021.009

HHMI Author Manuscript

HHMI Author Manuscript

HHMI Author Manuscript

3.3. Design of the Codebook

Before readout sequences and target sequences can be assembled to form the sequence of encoding probes, a codebook must be designed. The first step in codebook design is the choice of an encoding scheme that is appropriate for the experimental goals. We have utilized two different encoding schemes for MERFISH. The first scheme is a constant Hamming Weight code generated by keeping all binary barcodes from an existing HD4 code known as the Extended Hamming Code that contain only four `1' bits. We call this code the Modified Hamming Distance 4 code (MHD4). The 16-bit version of this encoding scheme contains 140 binary barcodes and is capable of identifying all two-bit errors and correcting any individual single-bit error. Alternatively, if the error correcting abilities of this code are not utilized, it can also detect three-bit errors. The advantage of this encoding scheme is the very high calling rate, ~80%, and low misidentification rates that it provides, as discussed in Section 2.4. In the second encoding scheme, we utilized a constant Hamming Weight code generated from all possible combinations of four `1' bits. This code has a minimum HD of 2 between all barcodes, so we refer to it as a Modified HD 2 code (MHD2). The benefit of this encoding scheme is that the reduced HD allows a much higher level of multiplexing for a given number of a bits—a 14-bit code contains 1,001 barcodes. However, the reduced HD produces a lower calling rate and a slight reduction in accuracy. Again, see Section 2.4.

Here we describe algorithms to generate both encoding schemes; however, we would encourage users to consider alternative encoding schemes, e.g. versions of those provided below with fewer or more bits or schemes with different Hamming Weight or HD, in order to find a scheme that best suits their experimental needs. Again, examples of algorithms to generate these codes as well as the barcodes for the published 16-bit MHD4 and 14-bit MHD2 codes are provided at http://zhuang.harvard.edu/merfish/.

3.3.1. Generation of the MHD4 Encoding Scheme—Here we present a method for generating sets of constant-weight-4 HD-4 (MHD4) barcodes for any number of bits. As an interesting aside, we note that the task of creating the optimal constant weight coding scheme — the encoding scheme that has the maximum possible number of barcodes given a specific HD — remains an unsolved problem. Thus, the algorithm that we present here likely does not produce a constant weight HD-4 code with the maximum possible number of barcodes given a specific number of bits. However, comparison of estimates of the upper bound on the number of barcodes possible in such codes (Brouwer and Etzion, 2011) and the number of barcodes generated by this algorithm suggests that it performs fairly well, typically producing ~75% of the possible number of barcodes. The 16-bit MHD4 code that we have produced is the rare exception: It contains 140 barcodes which is the current known upper limit for an MHD4 code of this length (Brouwer and Etzion, 2011).

Step 1: Generate the Extended Hamming Code that contains the desired number of bits. Details on how to generate this code are discussed many places online, and software to perform this calculation is included at http://zhuang.harvard.edu/merfish/.

Step 2: Select only barcodes with the desired Hamming Weight.

NanoString Exhibit 1021.010

HHMI Author Manuscript

HHMI Author Manuscript

HHMI Author Manuscript

3.3.2. Generation of the MHD2 Encoding Scheme—Constant weight HD2 codes are straightforward to generate, and the algorithm that we provide below will produce the optimal code, i.e. the maximum number of barcodes with four `1's and a minimum HD of 2.

Step 1: Generate a barcode of the desired length with only four `1's.

Step 2: Generate all possible permutations of the bits in this barcode.

3.3.3. Barcode Assignment—Once the desired barcodes have been designed, the codebook is designed by randomly associating each barcode with a specific RNA of interest. We recommend leaving 5-10% of the possible barcodes unassigned. These `blank' or `control' barcodes will serve as internal controls and will provide estimates of the frequency with which barcodes can be generated by background or spurious signals. The specific use of these `blank' measurements in discussed in Section 7.4.2 below.

3.4. Assembly and Screening of Encoding Probes

Once the target regions, the readout regions, and the barcodes associated with the desired encoding scheme are designed, the sequence of the encoding probes can be assembled. Each encoding probe will contain multiple readout sequences. However, given length restrictions in synthesis of these sequences, it is typically not the case that all of the readout sequences for each RNA will fit into each encoding probe. We use two readout sequences per encoding probe.

Step 1: Select the readout sequences for each encoding probe. For each possible target region, use the barcode assigned to that RNA to determine which readout sequences to use. We select the readout sequences that we use for each encoding probe randomly, without repeating a readout sequence more than once in a single encoding probe. We find that random assignment rarely produces issues with an imbalance in the usage of some readout sequences and negates concerns over potential biases that may arise from the position of the readout sequence in the encoding probe.

Step 2: Assemble the encoding probe. We place one readout sequence on either side of the targeting sequence though there is no reason why alternative arrangements could not be used. See Figure 2. Care must be taken to insure that the proper orientation of these sequences is used: the readout sequences are the reverse complement of the readout probes designed in Section 3.2. Thus, the encoding probe sequence must contain the reverse complement of these probe sequences. Similarly, the target region portion of the encoding probe must contain the reverse complement of the corresponding sequence of the target RNA.

3.5. Design of Priming Regions

The protocol that we use to make encoding probes that contain the sequences designed above (Section 4) require the addition of two priming regions to each probe. The optimal regions should have similar T_M, no contiguous stretches of the same nucleotide longer than three, and relatively narrow GC content. They should also have limited homology to each other and to non-priming regions of the encoding probes.

NanoString Exhibit 1021.011

HHMI Author Manuscript

HHMI Author Manuscript

HHMI Author Manuscript

Step 1: Truncate an orthogonal set of 25-nt long oligonucleotides to 20-nt. To generate possible primers that have limited possibility of binding to one another, we again start with the set of orthogonal 25mers designed by the Elledge lab as described in 3.2 Step 1. We reduce the length of these priming sequences to 20-nt to decrease the overall length of the final encoding probes.

Step 2: Screen oligonucleotides for ideal primer properties. We remove any potential primer with a T_M outside of the range of 70°C to 80°C as well as any oligonucleotide with any consecutive repeat of 3 or more identical nucleotides, which can create problems in the synthesis of the oligo. We also remove any oligonucleotide that does not contain a G or C in the final 2 nucleotides at the 3' end. The presence of this so-called GC clamp helps improve the efficiency and specificity of PCR primers.

Step 3: Screen the final set of possible primers for homology against the encoding probes. Finally, we use BLAST to identify stretches of homology within these primers and the encoding probes designed in Section 3.4. Any potential primer with a homology region of 11 nt or more is excluded.

Step 4: Add these primers to each encoding probe to form the template sequence for each oligonucleotide. The sequence of the primer that is added to the 3' end of the encoding probe should be the reverse complement of the sequence of the primer designed in Step 3. Table 2 contains an example of a template molecule for a single encoding probe.

Step 5: Screen assembled template sequences for homology to abundant RNAs. While individual components of these template molecules have been screened for homology against the transcriptome, it is possible that concatenation of the different component sequences will produce regions of homology that will allow the probe to bind to other RNAs. We recommend using BLAST to screen the set of probes designed in Step 4 for homology to abundant RNA species like rRNA and tRNA. For the human transcriptome these sequences can be found within the ncRNA fasta file at the Ensemble website as described in Section 3.1 Step 2. Similarly, highly abundant mRNAs can also be included in this screen if such abundance information exists. To identify regions of homology, generate a BLAST database for these sequences, and use BLAST to screen the potential encoding probes. We remove any encoding probe with homology regions longer than 14 nt.

Step 6: (Optional). Combine multiple oligo sets to fill a single pool of oligonucleotides. We typically purchase these oligonucleotides as complex oligonucleotide pools generated by array-based synthesis often from CustomArray (http://www.customarrayinc.com/). This company sells two different sizes of complex oligonucleotide pools—a pool with 12,472 unique sequences or a pool with 92,918 unique sequences. There are situations in which one set of encoding probes for one experiment does not fill an entire pool. In this case it is possible to combine multiple sets of encoding probes intended for different experiments in the same oligopool simply by assigning each a unique set of primers. However, when primers are designed for such combined pools, we recommend performing Step 3 with a BLAST database comprising all encoding probes that will be present in the single oligonucleotide pool not just those in each set of encoding probes.

NanoString Exhibit 1021.012

HHMI Author Manuscript

HHMI Author Manuscript

HHMI Author Manuscript

4. Probe Construction

Staining hundreds to thousands of RNA species each of which requires tens of unique encoding probes requires a very large number of unique oligonucleotide sequences. The sheer number of unique sequences makes traditional solid phase oligonucleotide synthesis prohibitively expensive in most cases. For example, assuming a modest cost of $0.10/base, an encoding probe length of ~100 nt, and the need for ~50,000 unique oligos for a single MERFISH measurement, the cost of the needed oligos would be $500,000! To circumvent this astronomical cost, we have developed a high-throughput approach to generating these probes which utilizes array-derived synthesis of complex oligonucleotide pools. These array-derived complex oligonucleotide pools that contain ~100,000 custom designed sequences can be purchased for only a few thousand dollars. The challenge to using these pools is that each individual sequence is provided in quantities far too small to be used directly for labeling. Thus, we developed an enzymatic amplification protocol to generate the encoding probes in high quantity sufficient for RNA FISH experiments using the array-derived complex oligonucleotide pools as templates.

The basic protocol involves four steps, which are described in detail in the following sections. First, the oligopool is amplified via PCR to create template molecules for *in vitro* transcription. Second, an *in vitro* transcription produces RNA from these template molecules as well as another ~100-fold amplification. Third, a reverse transcription reaction generates single-stranded DNA from this RNA. Fourth, the RNA template is removed via alkaline hydrolysis. We utilize an RNA intermediate for two reasons: i) *in vitro* transcription can produce very large quantities of nucleic acid in very small volumes, reducing the amount of material that must be used, and ii) the alkaline susceptibility of RNA allows it to be easily removed from the final DNA probes. Because this reaction involves the use of an RNA intermediate, we recommend using the higher standards of laboratory cleanliness often required for handling RNA. Specifically, all surfaces and pipettes should be cleaned daily using RNase removal solutions and separate stocks of all buffers should be kept solely for RNA work.

4.1. Required Reagents

The following protocols will require the following reagents

1. 20X EvaGreen (Biotium; 31000)
2. 2X Phusion hot start polymerase master mix (New England Biolabs; M0536S)
3. Tris-EDTA (TE) pH 8 buffer (Ambion; AM9849)
4. DNA binding buffer (Zymo Research; D4004-1-L)
5. DNA wash buffer (Zymo Research; C1016-50)
6. Oligo binding buffer (Zymo Research; D4060-1-40)
7. 100-μg capacity silicon columns (Spin-V; Zymo Research; D4003-2-48)
8. RNA binding buffer (Optional; Zymo Research; R1013-2-100)

NanoString Exhibit 1021.013

HHMI Author Manuscript

HHMI Author Manuscript

HHMI Author Manuscript

9. RNA prep buffer (Optional; Zymo Research; R1060-2-100)
10. RNA wash buffer (Optional; Zymo Research; R1003-3-24)
11. Quick HiScribe T7 polymerase kit (New England Biolabs; E2050S)
12. RNasin plus (Promega; N2611)
13. Maxima H- reverse transcriptase (ThermoScientific; EP0751)
14. 10 mM mix of dNTPs (New England Biolabs; N0447S)
15. 0.5 M EDTA (Ambion; AM9261)
16. 1 N NaOH (VWR; JT5635-2)
17. Nuclease-free water (Ambion; AM9932)
18. 100% Ethanol (KOPTEC; VWR; 89125-186)
19. D/RNAaseFree (VWR; 47751-044)
20. 1.5 mL LoBind tubes (Eppendorf; 022431021)
21. PCR tubes

The following protocols will require the following equipment

1. Table top centrifuge
2. qPCR machine or thermocycler
3. 37 °C incubator or water bath
4. 50 °C water bath
5. 95 °C water bath
6. Vacuum manifold (optional)
7. Gel electrophoresis equipment for poly-acrylamide gels (optional)
8. Vacuum concentrator (optional)

4.2. Amplification of *in vitro* Template

The first step in this protocol is to use PCR to amplify template molecules for the *in vitro* transcription. We recommend running this reaction as a limited-cycle PCR, i.e. monitor the status of the reaction in real time with a qPCR machine and remove the samples immediately before the final amplification plateau. We recommend limiting the number of PCR cycles because we have found that over amplification of complex libraries can produce molecules that miss-prime on other molecules, forming long concatemers that both reduce the yield of proper encoding probes and which could produce spurious signals.

Step 1: Design the primers. This PCR will not only amplify the library, it will also add the T7 promoter to these molecules to allow *in vitro* transcription of these templates. The sequence of the forward primer is the same as that designed in Section 3.5. However, the sequence of the reverse primer, also designed in Section 3.5, must include a T7 promoter,

NanoString Exhibit 1021.014

HHMI Author Manuscript

HHMI Author Manuscript

HHMI Author Manuscript

TAATACGACTCACTATAGGG, at the 5' end. Example primers can be seen in Table 3. The forward primer will also be used as the primer for reverse transcription in Section 4.4 below; thus, it is recommended to order this primer at a relatively large synthesis scale, such as 100 nmol or 250 nmol. The T7 promoter ends in a G-triplet, and the presence of a G quadruplet, i.e. four Gs in a row, often significantly lowers synthesis yields; thus, we recommend removing any 5'-terminal G nucleotides in the sequence of the reverse primer. The presence of the terminal G nucleotides in the T7 promoter region will serve as replacements for these nucleotides in the priming region. Resuspend forward primer to 200 μM and the reverse primer to 100 μM both in TE.

Step 2: Prepare the PCR. In a 1.7 mL Eppendorf tube, mix the following: 40 μL 20X Eva Green; 2 μL 200 μM forward primer; 4 μL 100 μM reverse primer; 1 μL of 80 ng/μL complex oligopool; 353 μL nuclease free water; 400 μL 2X Phusion hot start polymerase master mix. Aliquot 50 μL volumes into 16 PCR tubes.

Step 3: Amplify the template. Run the following protocol on a qPCR machine: 1) 98 °C for 3 minutes; 2) 98 °C for 10 s; 3) 65 °C for 10 s; 4) 72 °C for 15 s; 5) Measure the fluorescence of each sample. Repeat cycle steps 2 through 5 until the rate at which the sample amplifies decreases, which is a sign that it is approaching the final amplification plateau. Due to the complexity of these oligonucleotide pools, it is very unlikely that, once denatured, each molecule will find and rehybridize to its complement as opposed to partially hybridize with the common priming regions of a different molecule; thus, it is recommended that samples be removed after the elongation step—while the instrument is at 72 °C— and before it reaches the 98-°C-melting step of the next cycle. If a qPCR machine is not available, we recommend determining the appropriate number of cycles to run by quantifying the yield of small-scale PCR reactions run for different number of cycles.

Step 4: Purify the template. We utilize column purification to remove enzyme, nucleotides, and primers. In a 15 mL Falcon tube, mix the following: 800 μL of the PCR reaction generated in Step 3; and 4 mL of DNA binding buffer. Pull this mixture across a 100-μg capacity column using either a vacuum manifold or a centrifuge. Wash the column twice with 300 μL DNA wash buffer, spinning the column in a table top centrifuge at maximum speed for 30 s each time. Elute the template by adding 170 μL nuclease-free water to the column, transferring the column to a fresh 1.7 mL Eppendorf tube, and spinning at maximum speed for 30 s. Set aside 10 μL of this reaction for quality control.

Step 5: (Optional) Quality control for template reaction. Two important quality control steps can be performed at this point. First, it is useful to measure the concentration of the template with a spectrophotometer, such as the Nanodrop. The concentration should be between 10 ng/μL to 50 ng/μL. The second quality control step is gel electrophoresis and will be described in Section 4.4 Step 5 below.

4.3. *In vitro* Transcription

The second step of this protocol is a high yield *in vitro* transcription reaction that further amplifies the template molecules created in Section 4.2 as well as converts them into RNA.

NanoString Exhibit 1021.015

HHMI Author Manuscript

HHMI Author Manuscript

HHMI Author Manuscript

Step 1: *in vitro* transcription. In a fresh 1.7 mL Eppendorf tube, mix the following: 160 μL of the *in vitro* template created in Section 4.2; 176 μL of nuclease free water; 250 μL of the NTP buffer mix provided with the Quick HiScribe T7 polymerase kit; 25 μL of RNasin Plus; and 25 μL T7 polymerase (from the same HiScribe kit). Incubate the reaction in a 37 °C incubator for 12–16 hours. Often the reaction is complete after 6–8 hours, but it is typically convenient to leave this reaction overnight. Remove 20 μL for quality control.

Step 2: (Optional) Quality control for the *in vitro* transcription. To confirm that the *in vitro* transcription was successful, purify the reaction and measure its concentration with a spectrophotometer. To purify, mix 20 μL of the *in vitro* reaction with 30 μL nuclease-free water, 100 μL RNA binding buffer, and 150 μL 100% ethanol. Pass across a 100-ug-capacity spin column in a table top centrifuge. Wash this column once with 400 μL RNA prep buffer, and then twice with 200 μL RNA wash buffer, each time with a 30 s spin at the maximum speed of the table top centrifuge. Elute the RNA with 100 μL nuclease-free water. If successful, the concentration of the *in vitro* transcription should be between 0.5 μg/μL to 2 μg/μL. Purified RNA can also be run on a gel as described in Section 4.4 Step 5 below.

4.4. Reverse Transcription and Purification of Encoding Probes

In this step of the protocol, the large quantities of RNA produced by the high yield *in vitro* transcription are converted to single-stranded DNA using a reverse transcription reaction. This RNA template is then removed via alkaline hydrolysis, and the final encoding probes are purified and concentrated.

Step 1: Reverse transcription. To the unpurified *in vitro* transcription created in Section 4.3, add the following and mix well: 200 μL 10 mM dNTP mix; 120 μL 200 μM forward primer; 240 μL 5X Maxima buffer; 24 μL RNasin Plus; 24 μL Maxima H- reverse transcriptase. Incubate in a 50°C water bath for 1 hour. It is important to use a water bath, not an air incubator, to insure that the temperature of the sample rises to 50 °C quickly.

Step 2: Alkaline hydrolysis. Split the above reaction into two 1.7-mL Eppendorf tubes and add the following to each: 300 μL 0.5 M EDTA and 300 μL 1 N NaOH. Incubate in a 95°C water bath for 15 minutes.

Step 3: Purification of ssDNA probe. Combine the two aliquots above into a single 50 mL Falcon tube and add the following: 4.8 mL Oligo binding buffer and 19.2 mL 100% ethanol. Mix well and split equally between eight 100-μg capacity spin columns. Pull the sample across the columns with a vacuum manifold or via centrifugation. Wash the columns once with 750 μL DNA wash buffer. Elute the columns using 100 μL of nuclease-free water. Combine eluates and set aside 10 μL for quality control.

Step 4: Concentration of probe. Use a vacuum concentrator to dry the samples. This process could take several hours. Resuspend the dried pellet in 24 μL of nuclease-free water, or if desired, the hybridization buffer described in Section 5.1. Store probe at −20 °C and avoid unnecessary freeze-thaw cycles. If a vacuum concentrator is not available, it is also possible to concentrate the probe using ethanol precipitation.

NanoString Exhibit 1021.016

HHMI Author Manuscript

HHMI Author Manuscript

HHMI Author Manuscript

Step 5: (Optional) Quality control of *in vitro* template, RNA, and probe. We recommend running the *in vitro* template, the RNA, and the final probe on a 15% TBE-urea polyacrylamide gel to identify both RNase contamination and low conversion of the reverse transcription primer to full length probe. Large smearing both in the RNA band and the probe band can indicate RNase contamination. Failure to efficiently convert the reverse transcription primer into probe is revealed by a bright band running at the 20-nt length corresponding to the primer. Increasing the amount of RNA template in the reverse transcription often improves the fraction of primer converted into probe. We routinely obtain ~75% or greater incorporation of the reverse transcription primer into probe with the above protocol.

5. Sample Preparation and Staining

The preparation and staining of samples for MERFISH follows closely the typical protocols used for smFISH (Raj et al., 2008). However, there are a few places in which we have modified these protocols to optimize MERFISH staining. Again, RNase contamination can destroy samples, so care should be taken to work in an RNase-free environment.

5.1. Required Materials

The following protocol will require these reagents and buffers

1. Fixation buffer (4% PFA in 1XPBS)
    - **a.** 1 mL 32% paraformaldehyde (PFA; Electron Microscopy Sciences; 15714)
    - **b.** 0.8 mL 10X Phosphate Buffered Saline (PBS; Ambion AM9625)
    - **c.** 6.2 mL nuclease-free water
    - **d.** Store at −20°C in single use aliquots
2. Permeabilization buffer (0.5% v/v Triton X-100 in 1XPBS)
    - **a.** 5 mL 10X PBS
    - **b.** 45 mL nuclease-free water
    - **c.** 250 μL Triton X-100 (Sigma; T8787)
    - **d.** Store at room temperature
3. 2X SSC buffer
    - **a.** 5 mL 20X Saline Sodium Citrate (SSC; Ambion; AM9763)
    - **b.** 45 mL nuclease-free water
    - **c.** Store at room temperature
4. 1X PBS buffer

NanoString Exhibit 1021.017

HHMI Author Manuscript

HHMI Author Manuscript

HHMI Author Manuscript

   a. 5 mL 10X PBS
   b. 45 mL nuclease-free water
   c. Store at room temperature

5. 20% w/v Dextran sulfate
   a. In an RNase-free bottle (such as an empty nuclease-free water bottle), mix the following
   b. 100 g dextran sulfate (Fisher Scientific; bp1585100)
   c. 300 mL nuclease-free water
   d. Stir with a stir bar cleaned with D/RNaseFree while heating gently on a hot plate (37 °C) until dissolved
   e. Add nuclease-free water to produce a 500 mL total volume
   f. Store at room temperature

6. Encoding probe hybridization buffer
   a. 300 μL 100% deionized formamide (Ambion; AM9342)
   b. 500 μL 20% w/v dextran sulfate (above)
   c. 100 μL 20X SSC
   d. 90 μL nuclease-free water
   e. 1 mg yeast tRNA (Life Technologies; 15401-011)
   f. 10 μL 200 mM Vandyl Ribonucleoside Complex (VRC; New England Biolabs; S1402S)
   g. Store at −20°C

7. Encoding probe wash buffer
   a. 15 mL 100% deionized formamide
   b. 5 mL 20X SSC
   c. 29.5 mL nuclease-free water
   d. 0.5 mL 200 mM VRC
   e. Store at 4°C in the dark and use within a few days

8. 40-mm diameter, No. 1.5 coverslips (Bioptechs; 40-1313-0319)

9. 60-mm diameter, Cell culture petri dish (Corning; 353802)

10. 1” × 3” microscope slides

11. Parafilm (VWR; 52858-076)

12. Orange FluoSphere carboxylate-modified beads, 0.1-um-diameter (ThermoScientific; F-8800)

NanoString Exhibit 1021.018

HHMI Author Manuscript

HHMI Author Manuscript

HHMI Author Manuscript

The following protocol requires the following equipment

1. Equipment for cell culture
2. 37 °C incubator
3. 47 °C incubator
4. Laboratory rocker

5.2. Fixation and Permeabilization of Cells

The first step in most FISH protocols is to fix the cells and then to permeabilize the membrane using either an overnight incubation in 70% ethanol or a brief exposure to surfactant. We prefer the latter approach since this protocol requires less time; however, we have had reasonable performance with both approaches.

Step 1: Culture cells on a suitable coverglass. The culture substrate for cells should be the same coverglass that will be used for imaging. We utilize 40-mm diameter No. 1.5 coverslips from Bioptechs since these coverslips fit within the flow chamber that we use for imaging (discussed in Section 6). We typically culture cells in sterile, 60-mm-diameter petri dishes with one coverslip placed in the bottom of each dish.

Step 2: Fix cells. Allow the fixation buffer described in Section 5.1 to warm to room temperature. Aspirate culture medium from cells then gently decant 2-3 mL of fixation buffer into the petri dish that holds the coverslip. Cover and rock gently for 15 minutes at room temperature. Aspirate the fixation buffer and gently decant 2-3 mL of 1x PBS into the petri dish to wash the cells. Immediately aspirate this buffer. Repeat this 1XPBS wash for a total of three times.

Step 3: Permeabilize the cells. Aspirate any residual 1XPBS from the petri dish and decant 2-3 mL permeabilization buffer into the petri dish. Incubate the cells at room temperature with gentle rocking for 2 minutes. Aspirate out the permeabilization buffer and wash the cells three times with 1XPBS as described in Step 2.

5.2. Hybridization of Encoding Probes

Step 1: Exchange buffer on cells. Aspirate any residual 1XPBS, and gently decant 2-3 mL of room temperature encoding probe wash buffer into each petri dish. Rock the sample at room temperature for 5 minutes. This step insures that any residual buffer left on the coverslip will not significantly dilute the formamide in the hybridization buffer in the next step.

Step 2: Add hybridization buffer with probes. Place a layer of fresh parafilm on a 1” × 3” microscope slide. Dilute the encoding probes made in Section 4 into Encoding Probe Hybridization Buffer to the desired concentration, typically somewhere between 10 and 200 μM depending on the number of unique encoding probes in the probe set. Add 30 μL of this probe solution to the parafilm surface. Aspirate any residual encoding probe wash buffer from the coverslip and gently place the coverslip, cell-side-down, onto the droplet of encoding probes. Press gently to create a thin layer of encoding probe. The probe concentration needs to be optimized for each probe set: Higher probe concentrations

NanoString Exhibit 1021.019

HHMI Author Manuscript

HHMI Author Manuscript

HHMI Author Manuscript

produce brighter spots but a higher level of non-specifically bound probe background. We recommend titrating the concentration of probe across a ~40-fold concentration range (5 – 200 μM) to identify the concentration that produces the clearest signal relative to the background. We find that the optimal probe concentration only needs to be established once per probe set.

Step 3: Incubation. Create a humidity chamber by pouring nuclease-free water into the base of an old pipette tip box. Place the sample within this box and seal with parafilm. The sample will be sitting on the upper plastic level and should not come into contact with the water reservoir below. Place this box into a 37-°C incubation chamber and incubate for at least 12 hours. In some cases, we find that longer incubations (~36 hours) increase the quality of staining. Again, we recommend varying the incubation time for each probe set to identify the optimal incubation time.

Step 4: Wash away residual encoding probes. Preheat 6 mL of encoding probe wash buffer per sample to 47 °C in a water bath. Slowly peel the coverslip off of the microscope slide taking care not to crack the coverslip. If it appears to be stuck, immerse the assembly in a layer of encoding probe wash buffer for 5 minutes to loosen. Place the coverslip, cell-side-up, in a fresh 60-mm-diameter petri dish and add 3 mL of preheated encoding probe wash buffer. Place the petri dish in a 47 -°C incubator for 30 minutes. Aspirate the encoding probe wash buffer, add 3 mL of fresh encoding probe wash buffer, and repeat the 30-minute, 47-°C incubation. Aspirate the wash buffer and wash the sample in 2X SSC by adding 3 mL of 2XSSC and then immediately aspirating this buffer. Repeat this SSC wash for a total of three times.

Step 5: Addition of fiducial beads. Prepare a 100X solution of fluorescent beads by adding 10 μL of 0.1-nm-diameter Orange Fluospheres beads to 10 mL 2XSSC. Vortex to mix. This stock solution can be stored at 4 °C in the dark for several months. Further dilute this stock solution 1 to 100 in 2xSSC to create 3 mL of bead solution for each sample. Aspirate the 2XSSC from the samples and add the bead solution to each petri dish. Gently rock at room temperature for 15 minutes. We choose orange-colored beads (561-nm excitation) because we prefer to use the red imaging channel (641-nm excitation) for our smFISH images; however, the color of these beads could be changed to suit different imaging demands. We aim to have ~20 beads per field of view; thus, if different beads are used, the concentration should be adjusted to produce a similar final density of beads on the sample.

Step 6: Post-fixation. To fix the fiducial beads in place and to prevent subtle changes in the shape of the cell induced by the repeated washing that will occur in Section 6, we perform an additional fixation of the samples. Aspirate the bead solution and add 3 mL of fixation buffer prewarmed to room temperature to each petri dish. Gently rock the sample at room temperature for 10 minutes. Aspirate the fixation buffer, and wash the sample three times with 2xSSC. If the sample was prepared in an RNase-free environment, it can now be stored in 2XSSC at 4°C for several days. We do not recommend prolonged storage.

NanoString Exhibit 1021.020

HHMI Author Manuscript

HHMI Author Manuscript

HHMI Author Manuscript

6. MERFISH Imaging

The basic imaging process for MERFISH involves several fluid handling steps, e.g. introduction of hybridization buffers and wash and imaging buffers, in conjunction with the collection of smFISH images and the photobleaching of the sample. While it would be possible to perform these fluid exchange and imaging steps manually, we strongly recommend the use of an integrated and automated fluid exchange and imaging approach. Here we provide protocols for how to construct a fluid handling system that should be compatible with a variety of microscopes. We also discuss the basic protocols for hybridizing readout probes to samples on the microscope, imaging the sample, and bleaching residual signal.

6.1. Required Materials

The following protocols will require these reagents

1. Readout probe hybridization buffer
   - **a.** 25 mL 20% w/v dextran sulfate (Section 5.1)
   - **b.** 5 mL 20X SSC
   - **c.** 5 mL 100% deionized formamide
   - **d.** 14.5 mL nuclease-free water
   - **e.** 0.5 mL 200 mM VRC
   - **f.** Make fresh each day
2. Imaging buffer master mix
   - **a.** In an RNAse-free bottle (such as an empty nuclease-free water bottle) add the following
   - **b.** 50 mL 20X SSC
   - **c.** 25 mL 1 M TrisHCl pH 8 (Ambion; AM9856)
   - **d.** 325 mL nuclease-free water
   - **e.** 50 g glucose (Sigma; G8270)
   - **f.** A D/RNaseFree-treated stir bar
   - **g.** Stir until glucose is dissolved
   - **h.** Add nuclease-free water to 500 mL
   - **i.** Store at room temperature for up to a few weeks
3. Trolox solution
   - **a.** 20 mg (±)-6-hydrozy-2,5,7,8-tetramethylchromane-2-carboxylic acid (Trolox; Sigma; 238813)
   - **b.** 200 μL methanol (Sigma; 322415)

NanoString Exhibit 1021.021

HHMI Author Manuscript

HHMI Author Manuscript

HHMI Author Manuscript

   c. Make fresh each day

4. Imaging buffer
   a. 40 mL imaging buffer master mix
   b. 200 μL Trolox solution
   c. 200 μL catalase (Sigma; C30)
   d. 42 mg glucose oxidase (Sigma; G2133)
   e. Make fresh and use immediately
5. Photobleaching buffer
   a. 5 mL 20X SSC
   b. 44.5 mL nuclease-free water
   c. 0.5 mL 200 mM VRC
   d. Make fresh each day
6. Readout probe wash buffer
   a. 5 mL 2X SSC
   b. 10 mL 100% deionized formamide
   c. 34.5 mL nuclease-free water
   d. 0.5 mL 200 mM VRC
   e. Make fresh each day
7. Light mineral oil (Sigma; M5904)

Components for an automated fluidics system

1. Flow/imaging chamber (Bioptechs; FCS2)
2. 5”-long 20-gauge needles (Hamilton; 7750-11)
3. Luer to ¼-28 female fitting adaptor (IDEX; P-655)
4. 1/16” barb to ¼-28 female fitting adapter (IDEX; P-646)
5. ¼-28 fitting (IDEX; XP-202)
6. Clear ETFE tubing, 0.02” inner diameter (McMasterCarr; 5583K52)
7. Clear PVC tubing, 1/16” inner diameter (McMasterCarr; 5233K51)
8. 0.38-mm inner-diameter peristaltic tubing (Pulse Instrumentation; 116-0549-04)
9. Peristaltic pump (Gilson; Minipuls 3)
10. Computer-controlled valve (Hamilton; MVP; 36798)
11. 8-way valve (Hamilton; HVXM 8-5; 36766)

NanoString Exhibit 1021.022

HHMI Author Manuscript

HHMI Author Manuscript

HHMI Author Manuscript

12. 5 minute epoxy (VWR; 300050-778)
13. 25-gauge needles (VWR; BD305125)
14. 18-gauge needles (VWR; BD305196)
15. USB to RS-232 converter (Keyspan; USA-19HS)

The following protocol requires the following equipment

1. FCS2 flow system (Bioptechs; FCS2)
2. Objective heater (Bioptechs; 150803)
3. Automated flow system (see Section 6.2)
4. Microscope capable of smFISH imaging (see Section 6.3)

6.2. Assembly of and Operation of Flow System

Each round of MERFISH hybridization and imaging requires the controlled exchange of four different buffers at precise intervals. For this reason, integration of a fully automated fluid handling system with the microscope control software can significantly facilitate the collection of MERFISH data. Here we describe the construction and operation of the automated fluid system that we have used. This system is constructed around a peristaltic pump (Gilson; Minipuls 3) which controls the flow rate of different buffers through the flow system and a series of valves (Hamilton; MVP) that control which buffer is being pulled across the sample at any given time. The components required for the flow system are listed in Section 6.1, and a schematic diagram of the flow system required for 16-rounds of hybridization is included in Figure 4. Once assembled, the components of this flow system do not need to be replaced between measurements, unless otherwise specified.

Step 1: Assemble buffer reservoirs. Using an 18-gauge needle, create a hole in the cap of one 15 mL falcon tube for each hybridization round. In the example depicted in Figure 4, sixteen such tubes would be needed. Insert a 5”-long 20 gauge needle into each hole. Slide the needle so that it is ~ 1 mm from the bottom of the 15 mL falcon tube and use 5-minute epoxy to secure it. Using the same protocol, insert and secure a needle into the cap of three 50 mL falcon tubes (one each for the imaging buffer, wash buffer, and bleaching buffer). Connect a luer to ¼-28 fitting adapter to the end of each needle.

Step 2: Create a waste bottle. Using the same approach as described in Step 1, insert a needle into the top of a 1 L plastic bottle which will serve as waste collection. The collected waste from a MERFISH measurement will contain formamide and, thus, must be discarded as toxic waste. Choose a plastic bottle appropriate for this requirement.

Step 3: Assemble tubing for flow lines. Cut the ETFE tubing for each desired flow line using a fresh razor blade. Take care to make the end as flat as possible. The length of each tubing section should be as short as possible to reduce the dead volume within each flow line but long enough to allow easy manipulation of the component to which it is attached, such as a Falcon tube. Typical lengths are ~12”. Assemble a ¼-28 fitting on each end of each tubing section.

NanoString Exhibit 1021.023

HHMI Author Manuscript

HHMI Author Manuscript

HHMI Author Manuscript

Step 4: Assemble the flow lines. Insert the 8-way valve into each MVP valve system following the manufacturer's instructions. The valve system is going to be run as a daisy chain, so connect fluidics lines such that the first valve addresses the first seven hybridization buffers and the contents of the second valve system, the second valve system addresses the next seven hybridization buffers and the contents of the third valve, and the third valve addresses the remaining two hybridization buffers (assuming 16 rounds of hybridization) and the imaging, wash, and bleaching buffers. See Figure 4 for a flow diagram. This layout insures that when common buffers are flown across the sample, i.e. imaging, wash or bleach buffers, residual hybridization buffer from other rounds are not accidentally introduce into the sample.

Step 5: Connect flow lines to the FCS2 chamber. Flow connections are made to the FCS2 chamber via two metal tubes cast into this chamber. Cut two short sections of PVC tubing and gently slide these onto the metal tubes. Insert a 1/16” barb to ¼-28 female adapter into each PVC tube to allow flow lines to be connected to the flow chamber.

Step 6: Connect flow lines to the peristaltic tubing. Insert a 25-gauge needle into each end of the peristaltic tubing. Connect these needles to the ETFE tubing flow lines using luer to ¼-28 adapters

Step 7: Setup computer control. Both the peristaltic pump and the valve units can be controlled via serial communication. Most computers no longer contain serial ports, so we recommend using USB to serial converters such as a USB to RS-232 adapter as well as a RS-422 to RS-232 converter for the peristaltic pump. Custom software can be written to control these pumps via serial command; however, we have written a python-based graphical-user-interface program to control a pump and several valves. This software—named Kilroy in honor of the World-War-II-era character—is open source and can be found here: https://github.com/zhuanglab/storm-control. It can communicate with other software using TCP/IP, and, thus, it should be possible to integrate this fluidics control software with a wide variety of scripting languages available on many commercial microscopes.

6.3. Microscope Requirements

The physical requirements for a microscope for MERFISH measurements are essentially identical to the requirements for smFISH measurements. Even with many probes per RNA, the signal from individual RNAs is often relatively dim; thus, high numerical aperture objectives and sensitive cameras such as electron-multiplying CCD (EMCCD) or scientific CMOS are often needed. MERFISH requires relatively high laser powers to bleach the sample after each round of imaging; thus, the microscope should be able to illuminate the sample with at least 100 mW of light in the wavelength used to image the labeled RNAs, as measured at the back focal plane of the objective. Only a few mW of light is needed for illumination of the fluorescent fiducial beads. If less illumination light is available in the color channel used for smFISH, it should still be possible to perform MERFISH measurements. The user will simply need to devote more time to photobleaching each region of the sample. Finally, to achieve any reasonable level of automation and throughput with MERFISH, a motorized sample stage will be required as well as some form of automatic focus system.

NanoString Exhibit 1021.024

HHMI Author Manuscript

HHMI Author Manuscript

HHMI Author Manuscript

For published MERFISH measurements, we used a 1.45 NA, 100X oil immersion Olympus objective, and illuminated our sample with ~200 mW of 641-nm light and ~20 mW of 561-nm light, as measured at the back focal plane of the objective, using solid state lasers (MPB communications; VFL-P500-642; and Coherent, 561-200CWCDRH). The 641-nm laser was used to excite our Cy5-labeled readout probes while the 561-nm laser was used to excite the fiducial beads. A custom dichroic (Chroma, zy405/488/561/647/752RP-UF1) and a custom notch filter (Chroma, ZET405/488/561/647-656/752m) were used to couple this light into the objective and filter the emission. These custom optics were used so that our home-built microscope had the capability of imaging at 750-nm. This color band was not used in our published MERFISH work (Chen et al., 2015), and thus stock dichroics and emission filters would also have worked. For example, the Chroma 89016bs dichroic in combination with the Chroma ZET561/10x and ZET642NF notch filters would also work. The fluorescent signal from the sample was imaged onto an EMCDD camera (Andor; iXon-897) through a QuadView (Photometrics), which used several stock dichroics (Chroma, T560lpxr; T650lpxr, and 750dcxxr) and emission filters (Chroma; ET525/50m, WT59550m-2f, ET700/75m, HQ770lp) to image several different color channels onto different quadrants of the camera. The 640-nm channel, corresponding to our RNA signal, and the 561-nm channel, corresponding to our fiducial beads were excited and imaged simultaneously with this setup. The 750-nm channel allows future work to include probes of this color but again was not used in our published MERFISH work (Chen et al., 2015). However, it would also be possible to forego the use of a QuadView and image each color channel one at a time, using the selective excitation of each laser to discriminate the color channels corresponding to Cy5 and the fiducial beads. That being said, it is crucial that no offset be introduced between the image of the smFISH signal and the image of the fiducial beads; thus, the same dichroic filter cube should be used for both color channels. We collected images corresponding to a 40×40 μm field-of-view with a pixel size of 167 nm in the sample plane. Our sample position was controlled with a motorized stage (Marzhauser) and our focus was maintained with a home-built autofocus system consisting of an objective nanopositioner (Mad City Labs, Nano-F) whose position was locked to the position of a IR laser spot (940-nm) reflected off of the sample-coverslip interface and imaged with a CMOS camera (Thorlabs, uc480).

6.4. MERFISH Imaging Protocol

The general MERFISH imaging protocol involves the hybridization of each readout probe, a brief wash step to remove some of the non-specifically bound probe, imaging of the sample, and then photobleaching of the sample, before hybridization of the next readout probe.

Step 1: Prepare the microscope and the flow system. Preheat the objective using the Bioptechs objective heater to 37.0 °C for at least two hours before the start of the measurement. This increased temperature is required to favor the proper hybridization of readout probes to the readout sequences. Room temperature is also suitable if the concentration of formamide is increased to 30% v/v and 40% v/v in the readout probe hybridization buffer and the readout probe wash buffer, respectively. Prepare a 5 mL aliquot of Readout Hybridization Buffer as described in Section 6.1 for each round of hybridization and dilute a single readout probe (designed in Section 3.2) into each buffer to a final

NanoString Exhibit 1021.025

HHMI Author Manuscript

HHMI Author Manuscript

HHMI Author Manuscript

concentration of 10 nM. Prepare the imaging, wash, and bleaching buffers as described in Section 6.1. Load all buffers into the flow system. The imaging buffer is O_2 sensitive, so add ~5-10 mL of light mineral oil to the top of this buffer by decanting it into the 50 mL falcon tube holding this buffer. This oil layer prevents the diffusion of O_2 into this buffer during the course of the measurement. Connect the input flow line to the FCS2 channel directly to the exit line, bypassing the FCS2 system, and prime the flow system by flowing enough of each buffer to completely fill its specific flow line. Flush the system with bleaching buffer to ensure that no hybridization buffers will flow onto the sample once it is added. Inspect each connection to see if bubbles are forming. The presence of bubbles indicates a loose or faulty connection. Tighten the connector or replace the tubing. If flow rates appear to be lower than expected, replace the peristaltic tubing. We recommend replacing the peristaltic tubing every few measurements.

Step 2: Load the sample. Assemble the 40-mm coverslip containing the sample as prepared in Section 5 into the FCS2 flow system. Flow bleaching buffer through the tubes to fill the chamber with liquid. Inspect the flow chamber to insure that no air bubbles remain in the chamber. If bubbles are present, gentle agitation of the flow chamber, via tapping on the coverslip, can often dislodge them.

Step 3: Hybridize the first readout probe. Flow ~2 mL of the first readout hybridization buffer across the sample at a flow rate of 0.5 mL/min. This volume should be sufficient to fill the dead volume of the flow system and chamber as well as to exchange the volume of the chamber many times over. Stop the flow and incubate the sample in the first hybridization buffer for 15 minutes. If the quality of individual stains is low, increasing this hybridization time can sometimes improve the quality of the stain.

Step 4: Wash the sample. Flow ~2 mL of the readout wash buffer across the sample, again at a flow rate of 0.5 mL/min. Incubate the sample for 5 minutes.

Step 5 (Optional): Inspect the quality of the sample and select regions of interest. After the first readout probe is hybridized to the sample, it is often useful to pause the automated imaging and fluid handling program and visually inspect the quality of the sample. For new samples, it is often necessary to adjust the excitation light intensity so as to produce bright signal but not saturate the camera. Similarly, it can be convenient to examine the sample at this point to identify specific regions or cells to image. Before examining the sample, be sure to flow imaging buffer across the sample as described in Step 6 below. The brief exposure to light at this stage typically is insufficient to produce any significant photobleaching as long as the sample is immersed in imaging buffer.

Step 6: Image the sample. Flow ~2 mL of imaging buffer across the sample at 0.5 mL/min. When flow has stopped, collect an image in both the color channel corresponding to the labeled readout probes (e.g. 641-nm) and the color channel corresponding to the fiducial beads (e.g. 561-nm) for all desired fields of view. We utilize ~50 mW at the microscope back port to excite our Cy5-labeled readout probes, which corresponds to an average power density of ~1kW/cm^2, and we use ~5 mW at the microscope back port to excite the fiducial beads, which corresponds to an average power density of 100W/cm^2.

NanoString Exhibit 1021.026

HHMI Author Manuscript

HHMI Author Manuscript

HHMI Author Manuscript

Step 7: Bleach the signal from each region. Flow ~2 mL of the bleaching buffer across the sample at 0.5 mL/min. When flow has stopped, return to each field of view, turn up the illumination to the maximum value for the color channel corresponding to the labeled readout probes. Illuminate each sample for a sufficient time to completely photobleach the signal. For our measurements, this time was typically 3 s. In our measurements, we utilize 200 mW of 641-nm laser power at the microscope back port, which corresponds to a power density of ~4kW/cm^2. However, the bleaching rate will depend strongly on the illumination properties of each microscope, and the optimal bleaching time should be determined empirically for each microscope.

Step 8: Repeat steps 3–7 for the remaining hybridization rounds.

Step 9: Cleanup the system. When the experiment is complete, replace all buffers with nuclease-free water and flow 5 mL through each flow line. Store the flow lines and buffer reservoirs filled with deionized water to prevent the crystallization of salts within the flow system. If the mineral oil used to protect the imaging buffer has been accidentally introduced into the flow system, wash the affected lines with 5-10 mL of isopropanol and then nuclease-free water.

7. MERFISH Data Analysis

The basic decoding of MERFISH data—the identification of specific RNA species for each spot in the sample—consists of three basic steps. First, fluorescent spots must be identified in all images. Second, slight changes in the stage position between images of the same region from different hybridization rounds must be corrected. Finally, sets of fluorescent spots that occupy the same location in the sample must be decoded into binary barcodes, which, in turn, are decoded into the specific RNA species. After these RNAs have been decoded, there are a series of simple calculations that can often be performed on the measured barcodes to determine important parameters associated with the performance of the measurements, such as estimates of the binary errors made at each bit or the relative confidence that can be ascribed to the counts for each RNA species. In this section, we provide protocols for performing these basic computational tasks. Example software and data can be found at http://zhuang.harvard.edu/merfish/.

7.1. Identification of Fluorescent Spots

There are a variety of software packages and approaches to identifying the location and brightness of fluorescent spots in images. In principle, any of these approaches should work reasonably well for this initial stage of the analysis of MERFISH data. However, some of the more advanced algorithms for the identification of fluorescent spots have been developed in the context of localization-based super-resolution microscopy. In these measurements, there is a desire to be able to properly localize molecules that are close enough together that their fluorescent spots partially overlap. Depending on the local density of RNAs within the cell, the signal from different RNAs does occasionally overlap, necessitating the use of these more advanced spot finders. The algorithm we use—3D-daoSTORM—was developed in our laboratory (Babcock et al., 2012) and is an extension of the daoPHOT algorithm original developed for the analysis of astronomy data (Holden et al., 2011). 3D-daoSTORM is open

NanoString Exhibit 1021.027

HHMI Author Manuscript

HHMI Author Manuscript

HHMI Author Manuscript

source and can be found with documentation here: https://github.com/ZhuangLab/storm-analysis. In this Section, we describe the basic steps for the use of this software for finding fluorescent spots in MERFISH data.

Step 1: Data conversion. The first challenge associated with any analysis software will be to insure that the image data is in an appropriate format. Our data is typically stored in a custom file format. While conversion to this format is possible, we instead recommend converting data to the more commonly used tif format, which the 3D daoSTORM algorithm can process. Many microscopes can already save images as tif format, so conversion may not be necessary.

Step 2: Determine the appropriate intensity threshold for spot finding. The daoSTORM algorithm requires that a threshold be selected to determine whether a spot is bright enough to fit or not. It is useful to first run spot finding software for a range of thresholds to determine which value performs the best at discriminating between bright spots and low intensity spots, which are likely due to off-target binding of encoding or readout probes. The brightness of spots can differ between different hybridization rounds, so it is often worthwhile to explore different thresholds for different readout probes. In practice, it may be difficult to determine the optimal threshold for discriminating background spots and spots that correspond to RNAs by simple visual inspection. Thus, we recommend analyzing data with a range of thresholds and using an iterative approach to select the threshold that produces the best decoding of MERFISH data. This process is discussed in detail in Section 7.5 below.

Step 3: Batch analyze the data. Once an appropriate threshold has been selected, use this software to identify the location of potential molecules in both the smFISH images and the images of fiducial beads.

7.2. Correction of Image Offsets

Every time the microscopy stage returns to a given location there will be a slight offset, often no more than a single pixel or two. Nonetheless, this small offset can significantly degrade the ability to align fluorescent spots within images of the same sample stained with different readout probes. For this reason, in each round of hybridization, we collect an image of small fluorescent beads stuck to the surface of the sample. Because the location of these beads are fixed with respect to the sample, apparent differences between the position of these beads between different rounds of hybridization can be used to correct these small stage offsets. We perform this correction by using the positions of these beads to create affine transformations that map the position of each spot in each round of hybridization back to the coordinate system defined by the image collected in the first round of hybridization.

Step 1: Find fiducial bead centroids. We utilize the same spot fitting approach described in Section 7.1 to determine the location of the fiducial beads in the images of these beads corresponding to each round of hybridization.

Step 2: Create the affine transformations. For each field of view, load the locations of the fiducial beads in each round of hybridization. To use these beads as control points in the

NanoString Exhibit 1021.028

HHMI Author Manuscript

HHMI Author Manuscript

HHMI Author Manuscript

construction of affine transformation, each bead in one image must be associated with beads in another image. This can be accomplished by associating each bead with its nearest neighbor in the other image. However, this simple approach will fail if the offset between images is substantially larger than the average distance between beads within a single field of view since the nearest neighbor between images would likely correspond to a different bead. In this case, an initial crude offset can be found by using image cross correlation either with the original bead images or with a lower resolution image created from the 2D histogram of the bead positions. This crude offset can be used to correct the positions of these beads to sufficient accuracy to allow simple association of nearest neighbors, which then allows the construction of the final affine transformation. Using this approach, we can re-register different frames with a residual error of roughly 20 nm, much better than a single pixel.

Step 3: Correct the location of fluorescent spots. Once the affine transformations are calculated, apply these transformations to the locations of all found fluorescent spots in each smFISH image and save the revised locations.

7.3. Decoding Barcodes

Once all spots have been transformed to the same coordinate system, spots in different rounds of hybridization that occupy the same or similar physical locations within the sample should be associated to create the specific binary barcode associated with the putative RNA at that location in the cell. We have explored several different approaches to performing this association. Here we present the algorithm that has performed best in our hands. One advantage of this algorithm is that it requires only one parameter: the maximum distance between spots in different rounds of hybridization. Figure 3A–C illustrates the decoding of an example MERFISH data set.

Step 1: Create a list of all found spots. For a single field of view, create a list of the location of all spots in all rounds of hybridization. This algorithm will create an N-bit binary barcode for each of these spots.

Step 2: Construct a barcode for each found spot. . For each spot in the list created in Step 1, compute the distance to the nearest spot in each round of hybridization. This will create a vector of N distances. To convert this vector into a binary barcode, compare the ith distance to the maximum allowed distance (a parameter of this algorithm). If this distance is less than or equal to this maximum distance, assign a `1' to the ith bit of the barcode for this spot. Otherwise, assign a `0' to that bit. We use a maximum distance of 160 nm, i.e. one camera pixel. Practically, we found that a smaller maximum distance between spots tends to discard more real barcodes than false barcodes, despite the fact that we can resolve the centroid of each RNA spot to better than 160 nm. This observation may be due to the fact that the position of the centroid for the observed spot for a single RNA varies on average by ~100 nm between different rounds of hybridization—an effect that may be due to the finite cellular volume occupied by each RNA.

Step 3: Remove redundant barcodes. This algorithm creates a barcode for all spots in all rounds of hybridization, ignoring the fact that spots in different rounds will be combined to

NanoString Exhibit 1021.029

HHMI Author Manuscript HHMI Author Manuscript HHMI Author Manuscript

form individual barcodes. Thus, each barcode may be replicated in the results returned by Step 2. Redundant barcodes will share the same set of spots, and, thus, the average centroid of the spots that form a barcode will be unique for each barcode. Thus, to remove these redundant barcodes, we compute the average centroid of all spots that comprise each barcode and remove extra copies of barcodes that share the same centroid. . We perform this step because it is computationally faster to create redundant barcodes and then remove them in this fashion than to identify such barcodes as they are created.

Step 4: Associate each binary barcode with the RNA it encodes. Using the codebook designed in Section 3.3 create a look-up table that associates each encoded RNA with all binary barcodes that encode it. If the encoding scheme is not capable of error correction, then there will only be one binary barcode for each RNA. If, on the other hand, the encoding scheme allows error correction, then each RNA will have multiple binary barcodes that correspond to that word. For the purposes of calculating several properties associated with the basic performance of MERFISH, it is useful to create two look up tables: one that corresponds to the correct binary barcodes and one that corresponds to all binary barcodes that can be matched to an RNA after error correction. The use of two look up tables will allow each decoded RNA to be marked as an exact match, i.e. no error correction was applied, or an error corrected match.

7.4. Calculate MERFISH Performance

The basic performance of a MERFISH measurement can be quickly assessed from several quantities that can be calculated from the barcodes decoded in Section 7.3. Here we describe the calculation of these quantities and their interpretation.

7.4.1. The Per-Bit Error Rate—If the encoding scheme has the capacity to correct errors, then it will also have the ability to determine the bit at which the corrected errors occurred. Using this ability, it is possible to compute the average `1'➔`0' or `0'➔`1' error rates associated with each round of hybridization. These quantities can be very useful in diagnosing the performance of a MERFISH run. For example, a high `1'➔`0' error rate for one round of hybridization may indicate poor staining in that round or perhaps an inappropriately high threshold for spot fitting. Alternatively, a high `0'➔`1' error rate may suggest that the spot fitting threshold is too low for that round of hybridization. To calculate this quantity, compute the number of times each RNA species was measured correctly N_C and the number of times it was measured with a word that contains a single-bit error at each possible position N_i. Figure 5A illustrates these counts for two example barcodes. These two quantities can then be used to estimate the probability of flipping the ith bit via $N_i/(N_i + N_C)$. (See the Materials and Methods of Chen et al. for a derivation of this expression.) Once the probability of flipping each bit is calculated for each RNA, an estimate of the bit flipping probability for each round is calculated from the average across all genes. See Figure 5B for an example of these per-bit error rates.

7.4.2. Background Counts and the Confidence Ratio—As discussed in Section 3.3.3, we recommend leaving a few percent of the possible barcodes unassigned. Measurements of these `blank' or `control' barcodes can then serve as a simple measure of

NanoString Exhibit 1021.030

HHMI Author Manuscript

HHMI Author Manuscript

HHMI Author Manuscript

the background count rate in MERFISH and can be used to assign a qualitative degree of confidence to the observed counts for different RNAs.

Perhaps the most obvious use of these `blank' barcodes is to set a lower limit on the number of counts that can be trusted. For example, if an RNA-encoding barcode is counted fewer times than a `blank' barcode, then it might be reasonable to assume that the counts for this RNA are dominated by background counts and should not be trusted. However, this use of the `blank' barcodes provides an overly cautious measure of the rate of background counts because it does not properly take into consideration the way in which different binary barcodes are related to one another. For example, imagine that one `blank' word is counted more frequently than a barcode representing a low abundance RNA. If these two barcodes are separated by a large HD, i.e. these barcodes have very few `1' bits in common, then it is possible that the errors that produced observations of this `blank' barcode may not be relevant for the measurement of the barcode associated with the low abundance RNA.

To partially capture the relationship between different barcodes and improve estimates of the accuracy of different barcode measurements, we have developed a metric that we term the confidence ratio. This ratio is defined as the number of measured binary barcodes that exactly match the binary barcode for a given RNA over the sum of this number and the number of counts for all binary words that differ from this barcode in only one bit, i.e. the ratio of the blue bars to the sum of the blue bar and all red bars in Figure 5A. For an error-correcting encoding scheme, this quantity is simply the ratio of the number of times an RNA was observed without the application of error correction to the number that was observed with error correction applied. However, error-correction is not required to compute the confidence ratio. All that is required is that all barcodes are separated by at least a HD of 2.

To illustrate the usefulness of this ratio, consider the following scenario. Imagine that one specific hybridization round is particularly problematic, and the `1'➔`0' error rate for that round is higher than others. (As Figure 5B illustrates, there can be variation between errors rates in different rounds of hybridization). Then RNAs encoded with binary barcodes that contain a `1' in that bit will tend to have more single-bit errors. This will decrease the confidence ratio for these words by generating a larger proportion of counts for these single-bit errors. However, RNAs encoded with binary words that do not contain a `1' in that bit will not see an increase in the number of single-bit errors in this round, and the confidence ratio for these RNAs will not be lowered.

Finally, a word of caution: the confidence ratio does not imply a quantitative level of confidence in the counts for a RNA. For example, a ratio of 0.3 does not imply that 30% of the measured counts are correct. The proper interpretation of this ratio is more qualitative: one should trust the counts for a RNA with a confidence ratio of 0.5 more than those for a value of 0.3. To provide a heuristic cut-off on the confidence ratio, we use the measured confidence ratios for the `blank' barcodes. If an RNA-encoding barcode has a confidence ratio larger than the largest confidence ratio observed for the `blank' barcodes then we generally trust the counts associated with this RNA. See Figure 5C. Of course, this cut-off is still somewhat arbitrary, and we only recommend using it as a rule of thumb. The confidence ratio is one of the simplest quantities one could compute in an effort to exploit the natural

NanoString Exhibit 1021.031

HHMI Author Manuscript

HHMI Author Manuscript

HHMI Author Manuscript

geometric connectivity of the different measured binary barcodes. In the future, we expect that more complicated calculations could be performed to exploit this connectivity and further improve both the accuracy of the measured counts with MERFISH and our metrics of the performance of a given measurement.

7.5. (Optional) Iterative Identification of Optimal Thresholds

As discussed in Section 7.1, we observe that different rounds of hybridization produce somewhat different levels of background and spot brightness. Thus, it is typically advisable to tune the spot-finding threshold for each round of hybridization. To further improve this process, it is possible to automate this threshold search by using some of the performance metrics discussed in Section 7.4 to determine the optimal threshold for each hybridization round.

Step 1: Run the spot-fitting algorithm for a range of spot-brightness thresholds. We analyze each MERFISH data set with 10-20 thresholds spanning a range set by examining these data by hand.

Step 2: Select a starting set of thresholds and decode barcodes using these found spots. The initial thresholds can be selected at random or one can start at one limit—i.e. all thresholds are the lowest or highest possible values. With these found spots, run the decoding algorithm discussed in Section 7.3.

Step 3: Compute a quality metric. For the MHD4 code, where it is possible to calculate the per-bit error rates, we calculate the geometric mean of all `1'➔`0' and `0'➔`1' error rates. For the MHD2 code which does not have the ability to correct errors and calculate these per-bit error rates, we utilize the ratio of the number of barcodes with four `1' bits to those measured with three or five `1' bits, i.e. the average confidence ratio.

Step 4: Iterate. Repeat Steps 2 and 3 for a variety of threshold combinations, and select the threshold combination that maximizes the selected quality metric. Typically, we change our threshold combinations during each iteration round by selecting one hybridization round, fixing the threshold for all other rounds, and screening through all possible threshold values for this round. Once all thresholds have been screened for this round, we select the threshold value for that round that produces the highest quality metric and then fix this threshold value for this hybridization round for subsequent iterations. We then repeat this process for each subsequent hybridization round. Once we have screened the thresholds for all hybridization rounds in this fashion, we repeat this process, often for a total of three times. We find that both quality metrics that we have used typically converge with only a few iterations through all hybridization rounds. More complicated search strategies are also possible.

8. Summary

smFISH is a powerful technique because it allows the quantitative measurement of the exact copy number and spatial distribution of individual mRNAs within single cells in intact tissues. MERFISH extends these powerful abilities to the transcriptome scale by massively multiplexing smFISH measurements by encoding individual RNA species with error-robust

NanoString Exhibit 1021.032

HHMI Author Manuscript HHMI Author Manuscript HHMI Author Manuscript

barcodes and reading out the barcodes via a series of smFISH measurements. We anticipate this method to be relatively easily adopted by other laboratories and the techniques described in this chapter should facilitate these efforts as will the supporting protocols and code that can be found at http://zhuang.harvard.edu/merfish/.

Acknowledgments

We thank Guiping Wang, Kok Hao Chen, Siyuan Wang, Alistair Boettiger, and Junjie Hao for comments on the manuscript. This work was in part supported by the National Institutes of Health. J.R.M. was funded in part by a Helen Hey Whitney Postdoctoral Fellowship. X. Z. is a Howard Hughes Medical Institute Investigator.

References

Babcock H, Sigal YM, Zhuang X. A high-density 3D localization algorithm for stochastic optical reconstruction microscopy. Opt. Nanoscopy. 2012; 1:6.

Balagopal V, Parker R. Polysomes, P bodies and stress granules: states and fates of eukaryotic mRNAs. Curr. Opin. Cell Biol. 2009; 21:403–408. [PubMed: 19394210]

Batish, M.; Raj, A.; Tyagi, S. RNA Detection and Visualization. In: Gerst, JE., editor. Methods in Molecular Biology. Humana Press; Totowa, NJ: 2011.

Beliveau BJ, Joyce EF, Apostolopoulos N, Yilmaz F, Fonseka CY, McCole RB, Chang Y, Li JB, Senaratne TN, Williams BR, et al. Versatile design and synthesis platform for visualizing genomes with Oligopaint FISH probes. Proc. Natl. Acad. Sci. 2012; 109:21301–21306. [PubMed: 23236188]

Besse F, Ephrussi A. Translational control of localized mRNAs: restricting protein synthesis in space and time. Nat. Rev. Mol. Cell Biol. 2008; 9:971–980. [PubMed: 19023284]

Brouwer AE, Etzion T. Some new distance-4 constant weight codes. Adv. Math. Commun. 2011; 5:417–424.

Buxbaum AR, Haimovich G, Singer RH. In the right place at the right time : visualizing and understanding mRNA localization. Nature. 2014; 16:95–109.

Chen KH, Boettiger AN, Moffitt JR, Wang S, Zhuang X. Spatially resolved, highly multiplexed RNA profiling in single cells. Science. 2015; 348:aaa6090. [PubMed: 25858977]

Femino, a M.; Fay, FS.; Fogarty, K.; Singer, RH. Visualization of single RNA transcripts in situ. Science. 1998; 280:585–590. [PubMed: 9554849]

Holden SJ, Uphoff S, Kapanidis AN. DAOSTORM: an algorithm for high- density super-resolution microscopy. Nat. Methods. 2011; 8:279–280. [PubMed: 21451515]

Holt CE, Schuman EM. The central dogma decentralized: new perspectives on RNA function and local translation in neurons. Neuron. 2013; 80:648–657. [PubMed: 24183017]

Itzkovitz S, van Oudenaarden A. Validating transcripts with probes and imaging technology. Nat. Methods. 2011; 8:S12–S19. [PubMed: 21451512]

Jakt LM, Moriwaki S, Nishikawa S. A continuum of transcriptional identities visualized by combinatorial fluorescent in situ hybridization. Development. 2013; 140:216–225. [PubMed: 23175635]

Larson DR, Singer RH, Zenklusen D. A single molecule view of gene expression. Trends Cell Biol. 2009; 19:630–637. [PubMed: 19819144]

Lécuyer E, Yoshida H, Krause HM. Global implications of mRNA localization pathways in cellular organization. Curr. Opin. Cell Biol. 2009; 21:409–415. [PubMed: 19249199]

Levesque MJ, Raj A. Single-chromosome transcriptional profiling reveals chromosomal gene expression regulation. Nat. Methods. 2013; 10:246–248. [PubMed: 23416756]

Levsky JM, Shenoy SM, Pezo RC, Singer RH. Single-cell gene expression profiling. Science. 2002; 297:836–840. [PubMed: 12161654]

Lubeck E, Cai L. Single-cell systems biology by super-resolution imaging and combinatorial labeling. Nat. Methods. 2012; 9:743–748. [PubMed: 22660740]

Lubeck E, Coskun AF, Zhiyentayev T, Ahmad M, Cai L. Single-cell in situ RNA profiling by sequential hybridization. Nat. Methods. 2014; 11:360–361. [PubMed: 24681720]

NanoString Exhibit 1021.033

HHMI Author Manuscript

HHMI Author Manuscript

HHMI Author Manuscript

Martin KC, Ephrussi A. mRNA localization: gene expression in the spatial dimension. Cell. 2009; 136:719–730. [PubMed: 19239891]

Moon, T. Error Correction Coding: Mathematical Methods and Algorithms. Wiley; New York: 2005.

Munsky B, Neuert G, van Oudenaarden A. Using gene expression noise to understand gene regulation. Science. 2012; 336:183–187. [PubMed: 22499939]

Padovan-Merhar O, Raj A. Using variability in gene expression as a tool for studying gene regulation. Wiley Interdiscip. Rev. Syst. Biol. Med. 2013; 5:751–759. [PubMed: 23996796]

Raj A, van Oudenaarden A. Nature, nurture, or chance: stochastic gene expression and its consequences. Cell. 2008; 135:216–226. [PubMed: 18957198]

Raj A, van den Bogaard P, Rifkin SA, van Oudenaarden A, Tyagi S. Imaging individual mRNA molecules using multiple singly labeled probes. Nat. Methods. 2008; 5:877–879. [PubMed: 18806792]

Rodriguez AJ, Czaplinski K, Condeelis JS, Singer RH. Mechanisms and cellular roles of local protein synthesis in mammalian cells. Curr. Opin. Cell Biol. 2008; 20:144–149. [PubMed: 18378131]

Rouillard J-M. OligoArray 2.0: design of oligonucleotide probes for DNA microarrays using a thermodynamic approach. Nucleic Acids Res. 2003; 31:3057–3062. [PubMed: 12799432]

Sanchez A, Golding I. Genetic Determinants and Cellular Constraints in Noisy Gene Expression. Science. 2013; 342:1188–1193. [PubMed: 24311680]

Shaffer SM, Wu M-T, Levesque MJ, Raj A. Turbo FISH: a method for rapid single molecule RNA FISH. PLoS One. 2013; 8:e75120. [PubMed: 24066168]

St Johnston D. Moving messages: the intracellular localization of mRNAs. Nat. Rev. Mol. Cell Biol. 2005; 6:363–375. [PubMed: 15852043]

Xu Q, Schlabach MR, Hannon GJ, Elledge SJ. Design of 240,000 orthogonal 25mer DNA barcode probes. Proc. Natl. Acad. Sci. 2009; 106:2289–2294. [PubMed: 19171886]

Youk, H.; Raj, A.; Van Oudenaarden, A. Imaging single MRNA molecules in yeast (Elsevier Inc.). 2010.

Zenklusen, D.; Singer, RH. Methods in Enzymology. 2010. Analyzing mRNA Expression Using Single mRNA Resolution Fluorescent In Situ Hybridization; p. 641-659.

NanoString Exhibit 1021.034

HHMI Author Manuscript

HHMI Author Manuscript

HHMI Author Manuscript

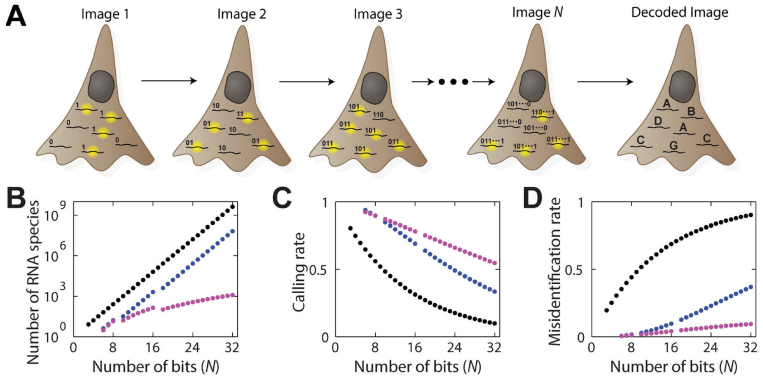

Figure 1.

Multiplexed, Error-Robust Fluorescence *in situ* Hybridization (MERFISH). (A) A schematic depiction of the process by which binary barcodes associated with each labeled RNA in a sample are readout. The presence or absence of fluorescence in each round of hybridization and imaging determines whether the barcode associated with each RNA in the sample has a `1' or `0' in the corresponding bit in the measured binary barcode. These barcodes are then used it identify each RNA, e.g. species, A, B, C, etc. (B) The number of RNA species that can be encoded with a binary barcode versus the number of bits N in those barcodes. A binary encoding scheme that utilizes all possible binary barcodes of length N is depicted in black. A binary encoding scheme that utilizes a subset of all possible binary barcodes that are all separated by at least a Hamming Distance of 4—an encoding scheme known as the Extended Hamming Code— is depicted in blue. A binary encoding scheme that utilizes a modified Hamming Distance 4 encoding scheme, which consists of all barcodes from the Extended Hamming Code that have a Hamming Weight of 4, i.e. only 4 `1' bits, is depicted in magenta. (C) The fraction of the binary barcodes that can be properly decoded into the correct RNA species—the calling rate— in the presence of modest readout errors as a function of the number of bits in the barcode for the same encoding schemes depicted in (B). (D) The fraction of binary barcodes that are misidentified as the wrong barcode and, thus, are decoded as the wrong RNA—the misidentification rate—as a function of the number of bits for the same encoding schemes depicted in (B). Panels (C) and (D) were calculated assuming an average `1'➔`0' error rate of 10% and a `0'➔`1' error rate of 4%, which correspond to the typical error rates observed in MERFISH measurements. Reproduced with permission from (Chen et al., 2015).

NanoString Exhibit 1021.035

HHMI Author Manuscript

HHMI Author Manuscript

HHMI Author Manuscript

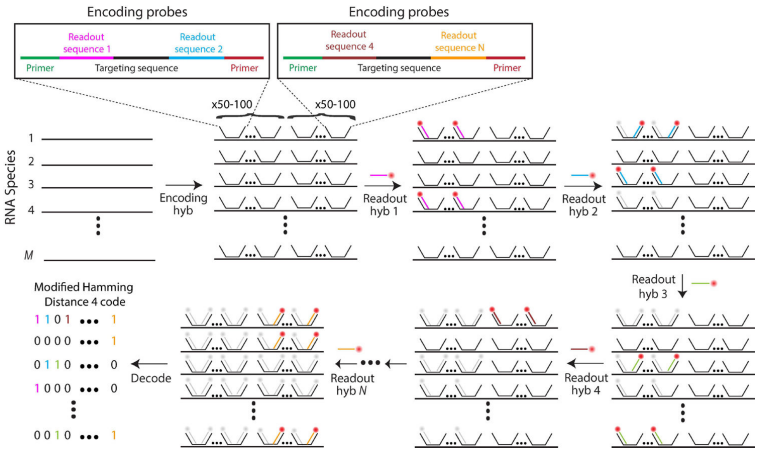

Figure 2.

Schematic depiction of the hybridization process used for MERFISH. Cellular RNAs are hybridized with a set of oligonucleotide probes, which we term *encoding probes*. These encoding probes contain a targeting sequence which directs their binding to the specific RNA. They also contain two readout sequences. For an experiment utilizing *N*-bit binary barcodes, *N* different readout sequences will be used with each bit assigned a different unique readout sequence. The specific readout sequences contained by an encoding probe to a given RNA are determined by the binary barcode assigned to that RNA: only the readout sequences assigned to bits for which this barcode contains a `1' are used. Each encoding probe also contains PCR priming regions used in its construction. To increase the signal from each copy of the RNA, multiple encoding probes, each with a different target region, are bound to the same RNA. The length of this *tile* of probes is typically between 50–100 probes. To identify the readout sequences contained on the encoding probes bound to each RNA, *N* rounds of hybridization and imaging are performed. Each round uses a unique, fluorescently labeled probe whose sequence is complementary to the readout sequence for that round. The binding of these fluorescent probes determines the bits which contain a `1', allowing the measurement of the specified binary code. Modified with permission from (Chen et al., 2015).

NanoString Exhibit 1021.036

HHMI Author Manuscript

HHMI Author Manuscript

HHMI Author Manuscript

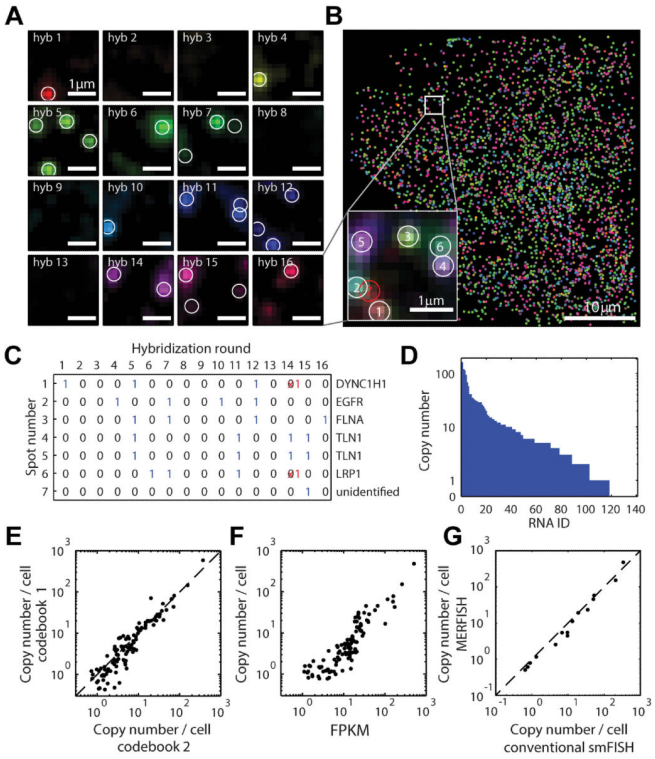

Figure 3.

Example MERFISH data for a 16-bit MHD4 Code. (A) smFISH images from each of 16 rounds of hybridization of a small field of view of a Human fibroblast (IMR90) stained with encoding probes utilizing an 16-bit MHD4 code that encodes 140 RNAs. The label depicts the readout hybridization round corresponding to each image. Circles correspond to the locations of identified fluorescent spots. (B) A single 40-μm-square field of view with all measured barcodes marked. The color of each marker represents the measured barcode. (Inset) An overlay of the small section of this field of view depicted in (A) with each set of overlapping spots labeled. White circles correspond to sets of spots that represent a barcode that can be decoded into a RNA while red represents a set of spots for which the measured barcode does not represent an RNA. (C) The measured binary barcodes for each set of spots in the small field of view depicted in (A) with the identity of the RNA represented by that barcode. Error correction was required for two barcodes in hybridization round 14 and is represented by red crosses. (D) The number of RNAs of each species identified in the single field of view depicted in (D). ~2000 RNAs were measured in this single field of view, and in a single measurement ~100 such fields of view containing 250,000 RNAs can be measured. (E) The average RNA copy number per cell measured with one implementation of the 16-bit MHD4 code versus the average copy number per cell for every RNA measured with another 16-bit MHD4 code in which each RNA was assigned a different barcode. The dashed line represents equality. (F) The average RNA copy number per cell versus the abundance as measured with bulk RNA-seq (FPKM). (G) The average copy number per cell measured via MERFISH versus that measured using conventional smFISH for 15 different RNAs. The dashed line represents equality. Panels reproduced with permission from (Chen et al., 2015).

NanoString Exhibit 1021.037

HHMI Author Manuscript

HHMI Author Manuscript

HHMI Author Manuscript

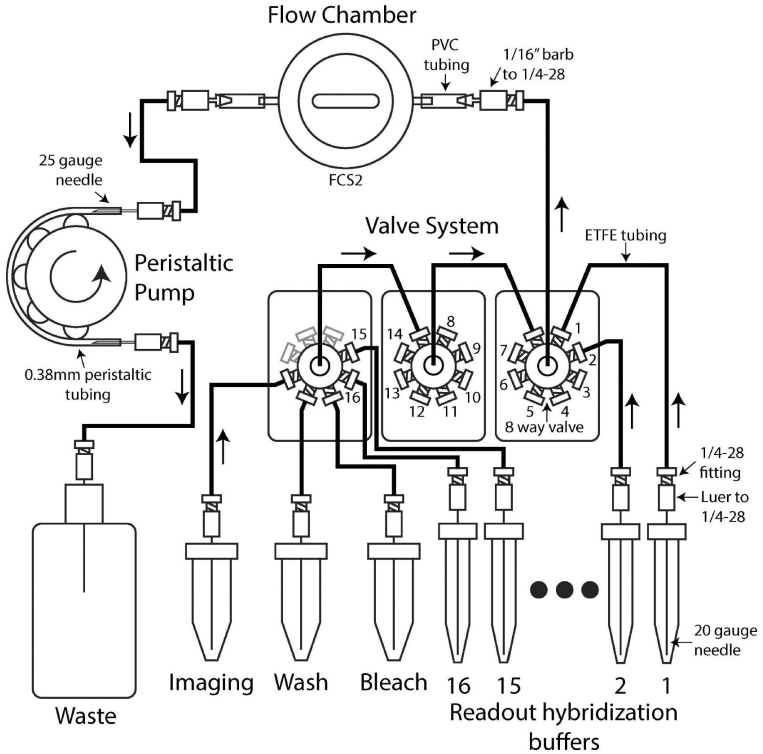

Figure 4.

Schematic diagram of the setup of an automated flow system for a 16-round MERFISH measurement. Arrows mark the local flow direction. For clarity, only 4 of the 16 tubes and flow lines required for the different hybridization buffers are depicted. The sample is contained within the FCS2 flow chamber.

NanoString Exhibit 1021.038

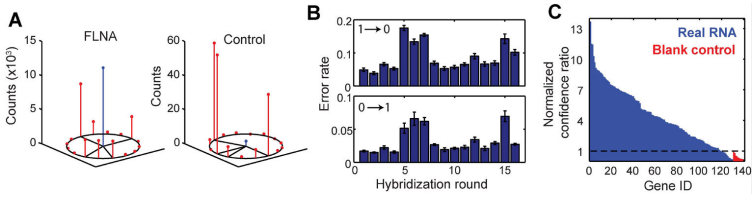

Figure 5.

MERFISH quality metrics. (A) Left: The number of molecule counts whose code exactly match that of FLNA (blue) and the number of molecule counts whose code differ in one bit from the FLNA barcode (red). (Right) as in (left) except for a barcode that was left intentionally unused to serve as a misidentification control (Control). Lines connecting the central exact counts to counts to barcodes that contain a single-bit error denote `1'➔'0' errors. (B) The average rate at which a `1' ➔ `0' (top) or `0' ➔ `1' (bottom) error occurs at each bit. These error rates are derived from the ratios of the counts to the correct barcode (A, blue) relative to the counts to the barcodes that differ in a single-bit (A, red). (C) The confidence ratio for each used barcode (Real RNA, blue) from a 16-bit, MHD4 measurement normalized to the largest confidence ratio observed for the `blank' barcodes (Blank control, red). All data are reproduced with permission from (Chen et al., 2015).

HHMI Author Manuscript
HHMI Author Manuscript
HHMI Author Manuscript
NanoString Exhibit 1021.039

HHMI Author Manuscript

HHMI Author Manuscript

HHMI Author Manuscript

Table 1

The sequence of the readouts probes that have been validated.

CGCAACGCTTGGGACGGTTCCAATCGGATC	CGCGAAATCCCCGTAACGAGCGTCCCTTGC
CGAATGCTCTGGCCTCGAACGAACGATAGC	GCATGAGTTGCCTGGCGTTGCGACGACTAA
ACAAATCCGACCAGATCGGACGATCATGGG	CCGTCGTCTCCGGTCCACCGTTGCGCTTAC
CAAGTATGCAGCGCGATTGACCGTCTCGTT	GGCCAATGGCCCAGGTCCGTCACGCAATTT
GCGGGAAGCACGTGGATTAGGGCATCGACC	TTGATCGAATCGGAGCGTAGCGGAATCTGC
AAGTCGTACGCCGATGCGCAGCAATTCACT	CGCGCGGATCCGCTTGTCGGGAACGGATAC
CGAAACATCGGCCACGGTCCCGTTGAACTT	GCCTCGATTACGACGGATGTAATTCGGCCG
ACGAATCCACCGTCCAGCGCGTCAAACAGA	GCCCGTATTCCCGCTTGCGAGTAGGGCAAT

NanoString Exhibit 1021.040

HHMI Author Manuscript

HHMI Author Manuscript

HHMI Author Manuscript

Table 2

An example template molecule for an encoding probe. The target region is marked with bold and italics, the readout sequences are marked with italics only, and the priming regions are marked with bold only. This encoding probe is to the VCAN RNA.

Encoding probe template	**CGCGGGCTATATGCGAACCG** *TTAGTCGTCGCAACGCCAGGCAACTCATGC* ***TAAAGAAATTAGATAGGCTGGAAATGCTTA*** *AAATTGCGTGACGGACCTGGGCCATTGGCC* **GCGTTGTATGCCCTCCACGC**

NanoString Exhibit 1021.041

HHMI Author Manuscript

HHMI Author Manuscript

HHMI Author Manuscript

Table 3

Example primers. These primers are compatible with the encoding probe template listed in Table 2. Note that the 5' G in the reverse primer has been removed so as not to create a G quadruplet with the terminal GGG of the T7 promoter.

Forward primer	CGCGGGCTATATGCGAACCG
Reverse primer with T7 promoter	*TAATACGACTCACTATAGGG* CGTGGAGGGCATACAACGC

NanoString Exhibit 1021.042